Multi-omics analysis reveals the differential mechanism of host growth and metabolism promotion by endophytic fungus and bacteria in *Atractylodes lancea*

Xiuzhi Guo[1,2#], Chengcai Zhang[1,2#], Yan Zhang[1,2], Sheng Wang[1,2], Ruishan Wang[1,2] , Jiancai Xiao[1,2], Yuefeng Wang[1,2], Zheng Peng[1,2], Yiheng Wang[1,2], Binbin Yan[1,2], Wanying Duan[1,2], Dehua Wu[1,2], Changzheng Liu[1,2], Feng Xiong[1,2], Hongyang Wang[1,2*], Chuanzhi Kang[1,2*] and Lanping Guo[1,2,3*]

[1] State Key Laboratory for Quality Ensurance and Sustainable Use of Dao-di Herbs, National Resource Center for Chinese Materia Medica, China Academy of Chinese Medical Sciences, Beijing 100700, China
[2] Key Laboratory of Biology and Cultivation of Herb Medicine, Ministry of Agriculture and Rural Affairs, Beijing 100700, China
[3] Institute of Chinese Materia Medica, China Academy of Chinese Medical Sciences, Beijing 100700, China
[#] Authors contributed equally: Xiuzhi Guo, Chengcai Zhang
[*] Corresponding authors, E-mail: wanghy@nrc.ac.cn; kangchuanzhi1103@163.com; glp01@126.com

Abstract

Microbial agents are expected to become effective tools for boosting both biomass and bioactive compound accumulation, to solve the challenges of poor quality and low yield in medicinal plants. Nevertheless, limited research has been conducted on the differential responses in plant growth and metabolism elicited by various types of endophytes, which constitute a significant natural microbial resource. In this study, the endophytic fungus *Paraphoma sp.* (F9) and the endophytic bacteria *Paraburkholderia aromaticivorans* (Pa) were inoculated into *Atractylodes lancea*. We found that both F9 and Pa exhibit a simultaneous enhancement on *A. lancea*'s growth and specialized metabolism. In fibrous roots, F9 notably increased biomass, root length, and flavonoid accumulation more than Pa. However, in rhizomes, the accumulation of medicinal terpenoids exhibited slight differences between F9 and Pa treatments. In both fibrous roots and rhizomes, F9 had a greater impact on gene expression changes in the *A. lancea* transcriptome compared to Pa. In fibrous roots, the flavonoid tricin-7-O-glucoside and genes (*CABs* and *LHC*) from the photosynthetic pathway, along with transcription factors (five *MYBs* and three *WRKYs*), showed a significant positive correlation. Thus, F9 has a greater effect on *A. lancea*'s photosynthesis, promoting better growth than Pa. In rhizomes, the terpenoid atractylon showed a strong positive correlation with genes, primarily enriched in immune response pathways. Therefore, most terpenoids exhibit comparable defense responses to various endophytes. This study will help optimize the utilization of endophyte resources in cultivating *A. lancea* and other plants.

Introduction

As global health care demand continues to increase, medicinal plant productivity must progress without exhausting critical environmental resources. Enhancing the quality and yield of these plants, along with optimizing their utilization, has therefore become a pressing issue[1]. Although chemical pesticides are effective, they carry considerable environmental and health risks[2], making it essential to identify suitable natural alternatives. Endophytes—vital components of medicinal plant microecology, consisting mainly of bacteria and fungi—can promote plant growth, improve host stress resistance, and facilitate active component accumulation[3]. Thus, endophytes play a beneficial role in host plant health and survival. Studies showed that diverse microorganisms distinctly influence the accumulation of plant metabolites such as alkaloids, phenols, and terpenoids[4]. This variation may be attributed to enzyme and gene expression, precursor supply, and hormone levels[4]. Understanding the mechanisms by which endophytes regulate plant metabolism and growth, will help optimize the use of microorganisms to improve both the quality and yield of medicinal plants.

Atractylodes lancea, a perennial herb, is primarily found in China, Japan, and Korea[5]. In traditional Chinese medicine, its rhizome is known for its ability to eliminate dampness, invigorate the spleen, dispel wind, and improve eyesight[5]. This therapeutic efficacy is intrinsically linked to the high content of volatile organic compounds (VOCs) primarily stored in the fibrous root and rhizome compartments. The main VOCs in *A. lancea* encompass terpenoid structures such as atractylon (CZT), hinesol (CZC), β-eudesmol (AYC), and polyacetylene structure atractylodin (CZS). These constituents collectively represent 71.30% of the total VOCs in the rhizome, whereas their content in the fibrous roots is markedly low[6]. Owing to the scarcity of wild resources, cultivated *A. lancea* has emerged as the predominant source in the market[7]. However, *A. lancea* has long faced significant cultivation challenges, including diseases and continuous cropping obstacles[8]. These challenges are also prevalent among other medicinal plants of the same category, severely diminishing their quality and yield[9]. In this context, endophytes, as a natural and valuable resource, may hold the key to effectively resolving these issues, and ensuring the sustainable production of medicinal plants.

It has been shown that the growth and metabolic processes of *A. lancea* are influenced by microbe incubation. Wang et al. found that soil microbe inoculation enhances *A. lancea* growth and VOCs accumulation[10]. Fang et al. demonstrated that endophytic fungus AL12 and AL4, as well as endophytic bacterium ALEB7B, augment total terpenoid accumulation[11,12]. They also determined

that fungal-induced terpenoids were regulated by phytohormones, including Jasmonic acid (JA), Salicylic acid (SA), Ethylene (ET), NO, and H$_2$O$_2$[13,14], while bacterial-induced terpenoids were regulated by Abscisic acid (ABA) and SA[15]. This suggests that endophytic fungi and bacteria may regulate terpenoid accumulation in *A. lancea* through distinct physiological mechanisms. Notably, previous research has predominantly focused on terpenoids in *A. lancea*. In recent years, the preponderance of extant research has been devoted to elucidating the interaction mechanisms between individual microbial strains and plants, as well as investigating the collective impact of microbial communities on plant growth[16–19]. In contrast, the differential effects of multiple microorganisms on the same host plant remain a relatively underexplored area in the current literature. This study therefore, selected *A. lancea* as the model species and comprehensively examined its differential responses to inoculation with endophytic fungi vs bacteria, providing a novel perspective on plant–endophyte interactions.

The rhizome and fibrous roots of *A. lancea* are key interfaces for microbial colonization. The changes in the characteristics of these compartments not only intuitively reflect the effects of *A. lancea*-endophytes interactions but are also crucial for elucidating the underlying mechanisms. Therefore, this study collects data from both the rhizome and fibrous root, to provide more comprehensive data support for the development of microbial inoculants for medicinal plants. Initially, the influence of the endophytic fungus F9 and the endophytic bacterium Pa on biomass production and the accumulation of VOCs in both the rhizome and the fibrous roots were systematically evaluated. Next, using metabolome analysis, the commonalities and differences in the differential accumulation of metabolites (DAMs) were compared between the F9 vs F9-free inoculation group and the Pa vs Pa-free inoculation group paired comparisons through comparative metabolomics in *A. lancea* rhizome and fibrous root. High-throughput sequencing was then utilized to identify differentially expressed genes (DEGs) in the *A. lancea* rhizome and fibrous root in response to F9 and Pa through comparative transcriptomics. The commonalities and differences in DEGs between the F9 vs F9-free inoculation, and Pa vs Pa-free inoculation comparison groups were further analazyed, performing KEGG analysis on the differentially expressed genes. Lastly, potential key metabolic pathways and genes significantly correlated with medicinal compounds, growth, and key DAMs were screened through matrix correlation and Pearson positive correlation analysis. This work uncovered the possible regulatory mechanisms of terpenoid and flavonoid biosynthesis, and accumulation, and improved our understanding of the interactions between the plant's key metabolites, transcriptome, and microbes in *A. lancea*, which could help guide future cultivation.

Materials and methods

Cultivation of plant material

A. lancea seeds were sourced from JinNiu-Dong-Shan (Mount Jin-Niu-Dong, coordinates: 31°46′37″ N, 119°18 ′52″ W) in Jintan City, Jiangsu Province (China). Following surface sterilization, the seeds were placed on Murashige and Skoog (MS) medium to facilitate the germination of surface-sterile plantlets. The aerial sections of the plantlets, measuring approximately 2–3 cm in height, were excised and cultured on solid MS medium (pH 5.8) supplemented with 30 g/L sucrose, 0.1 mg/L naphthalene acetic acid (NAA), and 1 mg/L 6-benzyladenine (6-BA) to promote vegetative propagation through tillering. Rooting was subsequently achieved by culturing *A. lancea* plantlets, which had been vegetatively propagated for four weeks,

and had reached a height of approximately 4 cm. Subsequently, *A. lancea* plantlets with approximately adventitious roots were removed from the rooting medium and planted in the sterile mixture (hereafter referred to as 'soil') of peat soil (Jiffy product, Netherlands), and vermiculite (6:1, v/v), then placed in a plant nursery room set at approximately room temperature (23 ± 2 °C, referred to as 'room temperature', RT hereafter) and with a 12 h/12 h light/dark cycle for seven days before being subjected to further treatments. This cultivation method was performed as per the method of Wang et al.[10].

Inoculation of endophytic strain Pa and F9

Our research group has isolated and identified six endophytic fungi and bacteria from the *A. lancea* rhizomes, and inoculated them into *A. lancea*. Through further screening, it was found that *Paraphoma* sp. (F9) in endophytic fungus, and *Paraburkholderia aromaticivorans* (Pa) in endophytic bacterium, exhibited the most significant effects on the growth promotion and quality enhancement of *A. lancea,* compared to the control group (Supplementary Fig. S1). And the effects were more stable (Supplementary Fig. S1). Therefore, this study selected these two strains for comparative research, aiming to explore the multifaceted differential responses of *A. lancea* to different endophytes. The data obtained will provide a scientific basis for the construction and optimization of microbial agents. Further, the protocol for the isolation and identification of endophytic fungi and bacteria is provided in the Supplementary material (Supplementary Protocol for Isolation and Identification of Endophytic Fungi and Bacteria). Endophytic bacterium Pa and endophytic fungus F9 were deposited in the China General Microbiological Culture Collection Center (CGMCC). The storage IDs were CGMCC No. 27816 for Pa, and CGMCC No. 41099 for F9. Pa was cultured in tryptose soya broth medium, and incubated at 37 °C for 48 h. The bacterial cells were collected by centrifugation, then resuspended in sterile water, and the OD600 value of the cell suspension was adjusted to 0.8–1.0 for *A. lancea* inoculation using a UV spectrophotometer. F9 was cultured in potato dextrose broth (PDB) (OXOID, UK) and incubated at 30 °C for seven days. PDB with F9 was filtered through sterile gauze to collect mycelia, and the spores were mixed with 10 mL of sterile water to form a 10^8 spore suspension. For inoculation, 10 mL of either F9 or Pa suspension was inoculated into the roots of *A. lancea* seedlings, referred to as the F9 and Pa groups, respectively. *A. lancea* seedlings treated with sterile water were used as the control group (CK). The experiment comprised five biological replicates, with three plants per replicate, for a total of 15 plants. The workflow schematic diagram is shown in Supplementary Fig. S2.

Sample collection and measurement of biomass

The samples were collected after 150 d. Every sample was divided into three parts: aerial part, rhizome, and fibrous root. Measurements encompassed the fresh weight of the whole plant (FW), the aerial portion (stem and leaf), the underground part (rhizome and fibrous root), and the length of the fibrous root. The dry weight of the underground part was determined after freeze-drying for one week, until a constant weight was achieved. A small portion of the fresh rhizomes and fibrous roots was retained for transcriptome sequencing. The samples were stored at −80 °C until sequencing. The dry samples were used for volatile medicinal compound detection and metabolome analysis.

Measurement of volatile medicinal compounds

The sample extraction followed previous methods[10]. A fine powder was made from freeze-dried rhizomes and root samples, with about 100 mg placed in 2 mL microcentrifuge tubes. Each tube received 500 μL of n-hexane, and ultrasound treatment at 60 Hz

for 15 min aided extraction. The mixture was then centrifuged at 5,000 × g at 4 °C for 5 min. The resulting supernatant was filtered through 0.22 μm polyethersulfone membrane filter capsules (Sterivex; Millipore) and prepared for analysis via gas chromatography-mass spectrometry (GC-MS). The hinesol, β-eudesmol, atractylon, and atractylodin contents in freeze-dried samples were measured via GC-MS using a Trace 1310 series GC with a TSQ8000 MS detector (Thermo Fisher Scientific Co. Ltd., Waltham, Massachusetts, USA), and a TR-5 ms capillary column (0.25 mm × 30 m, 0.25 μm). For the details of the detection method, please refer to Wang et al.[10]. The concentrations of the four volatile medicinal compounds in each sample were quantitatively determined using the external standard method (Supplementary Table S1).

Measurement and analysis of the metabolome

Samples were freeze-dried and ground into fine powder, with about 50 mg placed in 2 mL microcentrifuge tubes. The sample was mixed with 1,200 μL of a pre-chilled (−20 °C) 70% methanolic aqueous internal standard extract. The mixture was vortexed for 30 s every 30 min, six times. After centrifuging at 12,000 rpm for 3 min, the supernatant was filtered through a 0.22 μm membrane and stored in an injection vial for UPLC-MS/MS analysis.

UPLC-ESI-MS/MS system (UPLC, ExionLC™ AD) and a Tandem mass spectrometry system were used in the analysis of samples. An Agilent SB-C18 UPLC column (1.8 μm, 2.1 mm × 100 mm) was used for analysis, with the mobile phase consisting of solvent A (water containing 0.1% formic acid), and solvent B (acetonitrile containing 0.1% formic acid). Sample measurements used a gradient program starting at 95% A and 5% B, shifting linearly over 9 min to 5% A and 95% B, and held for 1 min. The mixture was reset to 95% A and 5% B in 1.1 min and held for 2.9 min. The experiment ran at a flow rate of 0.35 mL/min, with a column oven at 40 °C, and a 2 μL injection volume, using an ESI-triple quadrupole-linear ion trap (QTRAP)-MS for analysis. The ESI source parameters were set with a temperature of 550 °C, ion spray voltages of 5,500 V (positive), and −4,500 V (negative), ion source gases I and II at 50 and 60 psi, and curtain gas at 25 psi. High collision-activated dissociation was used. QQQ scans were conducted as MRM experiments with medium nitrogen collision gas. Declustering potential and collision energy were optimized for each MRM transition, and specific transitions were monitored based on the eluted metabolites. The raw metabolomic data obtained have been included in Supplementary Table S2. In metabolome analysis, differentially accumulated metabolites (DAMs) were identified using criteria of $|\log_2(\text{fold change})| \geq 1$ and $p < 0.05$. The relevant information on hormone detection was collated, as shown in Supplementary Table S3.

RNA extraction and transcriptome sequencing

Fresh samples were ground in liquid nitrogen, and 100 mg of the ground powder was used for RNA extraction with Trizol reagent (Thermo Fisher Scientific, Waltham, MA, USA) according to the manufacturer's instructions. An agarose gel electrophoresis was used to determine the integrity of the RNA, and a Nanodrop 2000 spectrophotometer was used to determine the purity of the RNA. A total of 0.5 g of RNA from each sample was reverse-transcribed into single-stranded cDNA using the PrimeScript RT Reagent Kit and gDNA Eraser (Takara Bio, Kusatsu, Japan). The synthesis of second-strand cDNA was carried out utilizing DNA polymerase, RNase, and dNTPs. AMPure XP (Beckman Coulter, Inc., Brea, CA, USA) was used for purification following end-repair, A-tailing, and adapter ligation. cDNA libraries were then constructed and diluted to 1.5 ng/μL for insert size assessment using an Agilent 2100 Bioanalyzer. RNA sequencing (RNA-seq) was conducted using the Illumina NovaSeq 6,000 platform (Illumina, USA).

Transcriptome data analysis using bioinformatics techniques

Gene functions were deduced using annotations from the KEGG, SwissProt, and Pfam databases[20]. Gene expression levels were measured using FPKM values. Principal component analysis (PCA) was conducted on all treatment groups using the NovoMagic website by Novogene. Differential expression analysis was conducted on representative samples, each with three biological replicates, using the DESeq2 package in R[21], with a negative binomial generalized log-linear model. Differentially expressed genes (DEGs) were identified using an adjusted p-value threshold of less than 0.05, and an absolute log2 fold change greater than KEGG analysis was performed using the clusterProfiler package in R[22], identifying pathways as significantly enriched at $p < 0.05$.

Detection of transcriptional expression levels of key genes

The RNA was transcribed into cDNA. Differential gene-specific primers were utilized for RT-qPCR using SYBR Green I, a double-stranded chimeric fluorescent dye method. Supplementary Table S4 contains the details of the gene-specific primers. The internal reference gene EF1α was used, and the average of three biological replicates was calculated. Gene expression was quantified via the $2^{-\Delta\Delta CT}$ method[23]. The primers used for EF1α amplification were 5′-CAGGCTGATTGTGCTGTTCTTA-3′ and 5′-TGTGGCATCCATCTTGT-3′, yielding a 241 bp product.

Statistical analyses and graphic visualization

Data recording and processing were carried out using Excel (Office 16). Graphical rendering utilized GraphPad Prism 8.0.1 (GraphPad Software Inc., USA). One-way ANOVA and Pearson correlation analysis were conducted using IBM SPSS Statistics 19.0 (SPSS, Chicago, IL, USA). Results are presented as mean ± standard deviation (SD). Venn analysis[24] and PCA[25], OPLS-DA[26], heatmap[27], and matrix correlation[28] were conducted using Metware Cloud (https://cloud.metware.cn), a complimentary online data analysis platform.

Results

Inoculation of endophytic fungus F9 demonstrated superiority over bacteria Pa in promoting root length

To evaluate the effects of endophytic fungus F9 and bacteria Pa on *A. lancea*'s growth, morphological traits were observed. Inoculated *A. lancea* showed noticeable morphological variations compared to uninoculated plants (Fig. 1a). Both endophytic strains Pa and F9 significantly increased the total fresh weight (FW) of *A. lancea* compared to the control (CK) (Fig. 1b). This increase was primarily from the FW of the underground parts rather than the aerial parts (Fig. 1c, d). The trend in dry weight after freeze-drying was consistent with fresh weight trends before drying (Fig. 1d, e). The F9 inoculation group (F9) exhibited slightly superior biomass increase compared to the Pa group (Pa). Additionally, the root lengths (RL) of plants inoculated with F9 and Pa differed significantly from CK, with the impact of F9 being greater than that of Pa (Fig. 1f). The trend in the change of chlorophyll a/b ratios and underground fresh weight was similar (Fig. 1g). Therefore, both F9 and Pa significantly increased underground biomass and chlorophyll a/b ratios in *A. lancea*, with similar enhancement effects observed between the two treatments. However, F9 exhibited a more pronounced promoting effect on root length, compared to Pa.
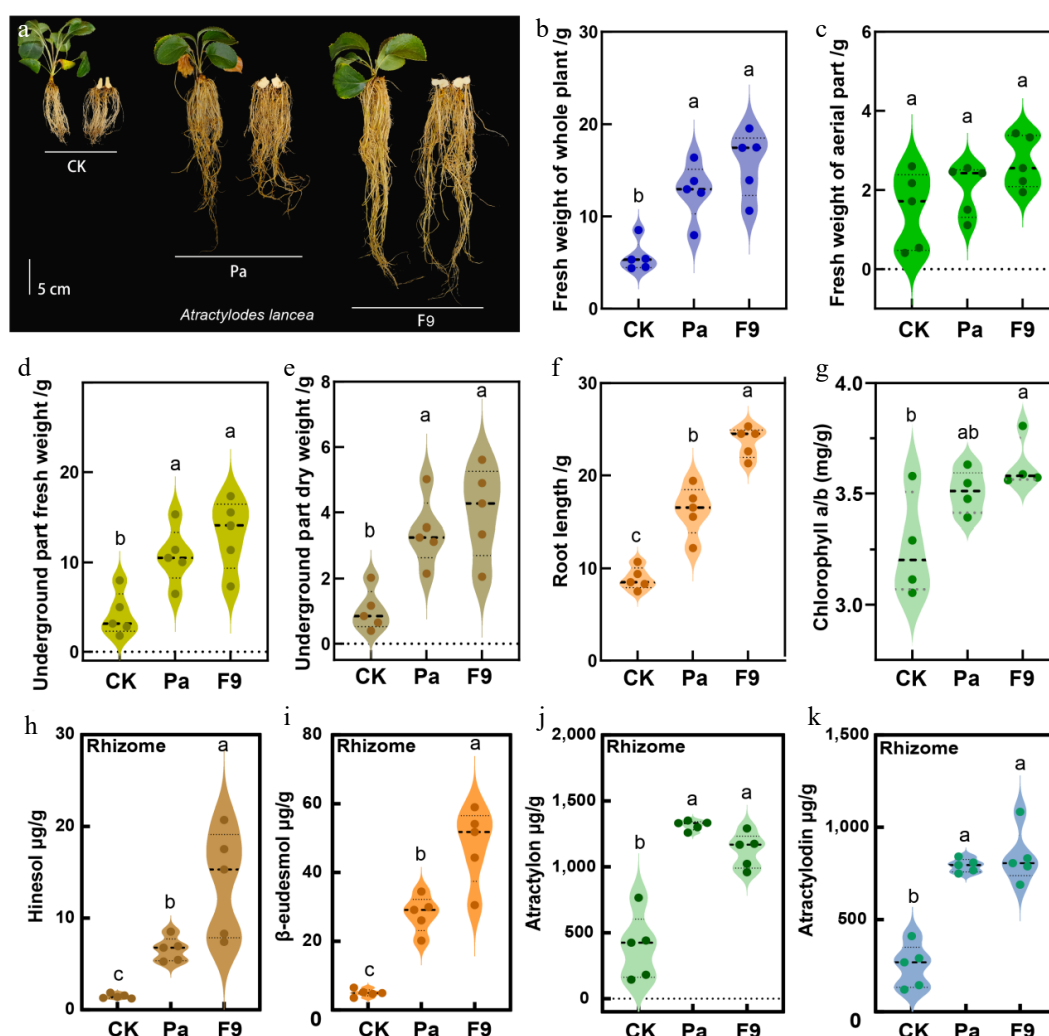
Fig. 1 The effect of inoculation with F9 and Pa on traits of *A. lancea*. The changes in (a) morphology and (b) fresh weight of the whole plant, (c) aerial part fresh weight, (d) underground part fresh weight, (e) underground part dry weight, (f) root length, (g) chlorophyll a/b ratio. The concentration of four medical compounds in *A. lancea* rhizomes, including (h) hinesol, (i) β-eudesmol, (j) atractylon, and (k) atractylodin, caused by F9 and Pa inoculation are shown. Different lowercase letters indicate significant differences (one-way ANOVA, $p < 0.05$, n = 5).

Synthesis of different volatile medicinal compounds has differential responses to fungal F9 and bacterial Pa

To explore the effect of F9 and Pa inoculation on medicinal compounds accumulation in *A. lancea* rhizome and fibrous root, hinesol, β-eudesmol, atractylon, and atractylodin were measured by GC-MS. In *A. lancea* rhizome, F9 inoculation significantly increases hinesol, β-eudesmol, atractylon, and atractylodin concentrations by 9.4-, 9.6-, 2.9-, and 3.4-fold compared to the control (Fig. 1h–k). Note that the concentrations of atractylon (731.8 μg/g), and atractylodin (592.9 μg/g) were significantly increased compared to those of hinesol (12.4 μg/g), and β-eudesmol (43.0 μg/g) (Fig. 1h–k). After inoculation with Pa, the levels of all four compounds similarly increased over the control, showing fold increases of 4.5, 5.6, 3.4, and 3.2, respectively. Furthermore, atractylon (924.1 μg/g) and atractylodin (545.6 μg/g) concentrations exceeded those of hinesol (5.1 μg/g) and β-eudesmol (23.0 μg/g) (Fig. 1h–k). Therefore, this indicated that the atractylon and atractylonin accumulation occurs more rapidly than that of hinesol and β-eudesmol over a given period. Additionally, both F9 and Pa inoculation similarly promoted the accumulation of atractylon and atractylodin (Fig. 1j, k), while F9 had a stronger effect on hinesol and β-eudesmol accumulation compared to Pa (Fig. 1h, i).

In the fibrous roots, only hinesol and atractylon were significantly induced by F9 and Pa, though their concentrations remained low (< 10 μg/g) (Supplementary Fig. S3). Hinesol and atractylon concentrations increased by 1.72- and 1.71-fold with Pa inoculation, and by 1.40- and 1.13-fold with F9 inoculation, respectively, as compared to controls.

In summary, both F9 and Pa inoculations similarly influence atractylon and atractylodin accumulation in the rhizome. However, the changes in hinesol and atractylon in fibrous roots, and in hinesol and β-eudesmol in rhizome, are affected by differences in endophytes types.

Comparison of the effects of F9 and Pa inoculation on the metabolome in *A. lancea* rhizome and fibrous root

To explore the impacts of endophytic strains F9 and Pa on *A. lancea*'s metabolic compounds beyond the medicinal compounds, UPLC-MS/MS detection and metabolome analysis were conducted on *A. lancea* rhizomes and fibrous roots. 1,572 compounds were identified, categorized into 13 class I, and 54 class II (Supplementary Table S5). Of these, 1,100 compounds, including flavonoids, amino acids and derivatives, phenolic acids, lipids, and terpenoids, were in the top 6 of class I, constituting over 60% of the total compounds (1,572).

In the rhizomes (r), there were significant differences between treatments with and without F9 (F) or Pa inoculation (Fr vs CKr or Par vs CKr) (Supplementary Fig. S4a), as well as between F9 and Pa inoculation groups (Supplementary Fig. S4b) by PCA analysis. Pairwise comparisons identified 678 differential accumulation metabolites (DAMs) with |$\log_2$Foldchange| > 1 and p < 0.05 (Supplementary Fig. S4c). To detail the response of each DAM to F9 and Pa, Venn (Supplementary Fig. S4d) and heatmap plots (Supplementary Fig. S4e−h) were generated from these 678 DAMs. Among them, 431 DAMs were common to CKr vs Fr and CKr vs Par, but not to Fr vs Par (Supplementary Fig. S4d). This suggested that F9 and Pa have similar effects on most DAMs in rhizomes. Of these 431 DAMs, downregulated compounds outnumbered upregulated ones (Supplementary Fig. S4g). Downregulated components primarily included amino acids and derivatives (91 compounds), while upregulated ones included terpenoids (21 compounds), amino acids and derivatives (20 compounds), and flavonoids (18 compounds) (Fig. 2a). Terpenoids with medicinal value. were further analyzed Among the terpenoids, seven of the top 10 showed increased results compared to the control, unaffected by F9 and Pa strains (Fig. 3a). Additionally, as hormones are a key endogenous factor

affecting plant secondary metabolism, hormone levels influenced by F9 and Pa inoculation were examined (Fig. 3b). Results showed consistent hormone level changes due to F9 and Pa, with the exception of phenyl salicylate (Fig. 3b). Notably, sulfo jasmonate and methyl dihydrojasmonate (2H_MeJA) responded to F9 and Pa were significantly enhanced. Overall, both F9 and Pa consistently enhanced the accumulation of the majority of compounds in the rhizome, significantly promoting the synthesis of seven out of the top 10 terpenoids, and two jasmonic acid derivatives.

In the fibrous roots (fr), PCA revealed significant differences between samples with and without F9 or Pa inoculation (CKfr vs Ffr or CKfr vs Pafr) (Supplementary Fig. S5a), and between the F9 and Pa inoculation groups (Supplementary Fig. S5b). Total number of DAMs with |$\log_2$Foldchange| > 1, p < 0.05 in pairwise comparisons, including Ffr vs CKfr, Pafr vs CKfr, and Ffr vs Pafr, was 681 (Supplementary Fig. S5c). To examine the trends of DAMs among Ffr, Pfr, and CKfr, Venn and heatmap plots for these 681 DAMs were generated (Supplementary Fig. S5c−f). F9 inoculation resulted in a greater number of upregulated compounds (Supplementary Fig. S5d, S5g, S5f) in *A. lancea* fibrous roots, compared to Pa inoculation (Supplementary Fig. S5d, S5h, S5f). Conversely, the combination of F9 and Pa
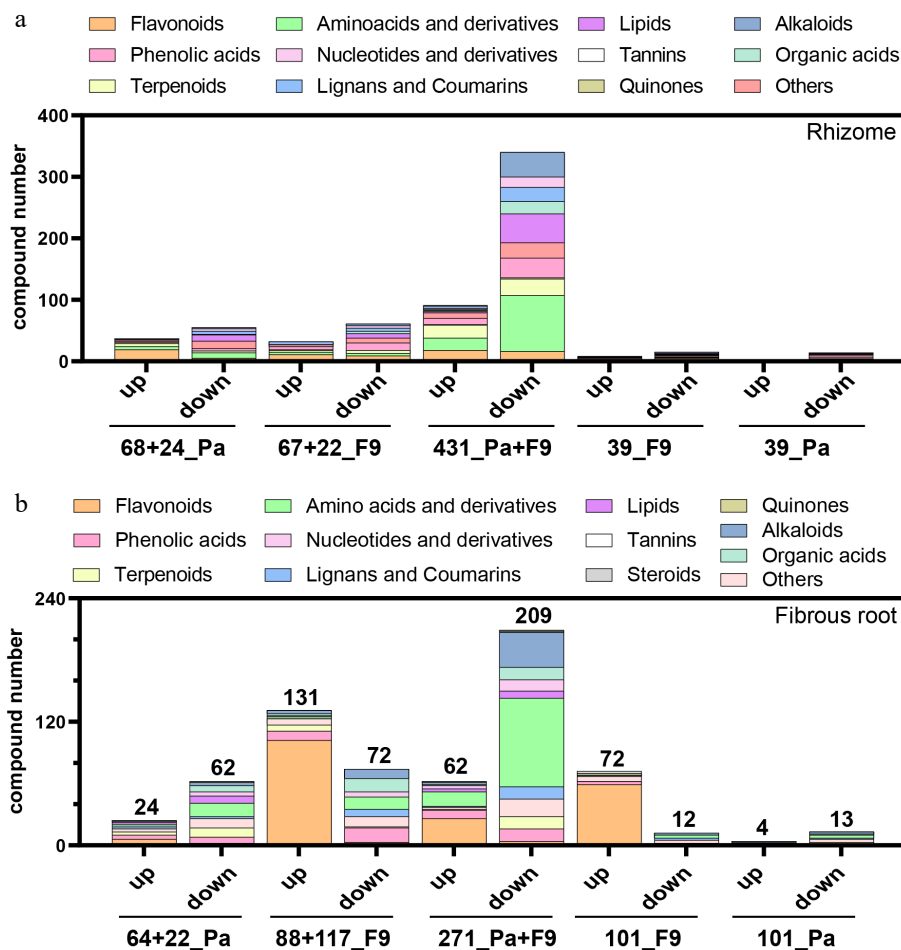

Fig. 2 The distribution of differentially accumulated metabolites (DAMs) in *A. lancea* (a) rhizomes, or (b) fibrous roots, caused by inoculation with F9 and Pa. (a) 68+24_Pa: the distribution of 92 (68+24) DAMs specifically associated with Pa treatment. 67+24_F9: the distribution of 91 (67+24) DAMs specifically associated with F9 treatment. 431_Pa+F9: the distribution of 431 common DAMs that were influenced by F9 treatment and Pa treatment compared to the control (CK). 39_F9 and 39_Pa: the distribution of 39 DAMs specifically caused by F9 or Pa inoculation, which obtained by pairwise comparison (F9r vs CKr, Par vs CKr, and Par vs F9r). The above numbers for (a) refer to Supplementary Fig. S4. (b) The meaning represented by the horizontal axis from left to right is the same as that in (a) except that the samples in (b) comes from *A. lancea* fibrous roots instead of the rhizomes. The above numbers for (b) refer to Supplementary Fig. S5. 'r', rhizome; 'fr', fibrous root; 'up', metabolite contents increased by F9 treatment or Pa treatment compared to the control; 'down', metabolite contents reduced by F9 treatment or Pa treatment compared to the control.
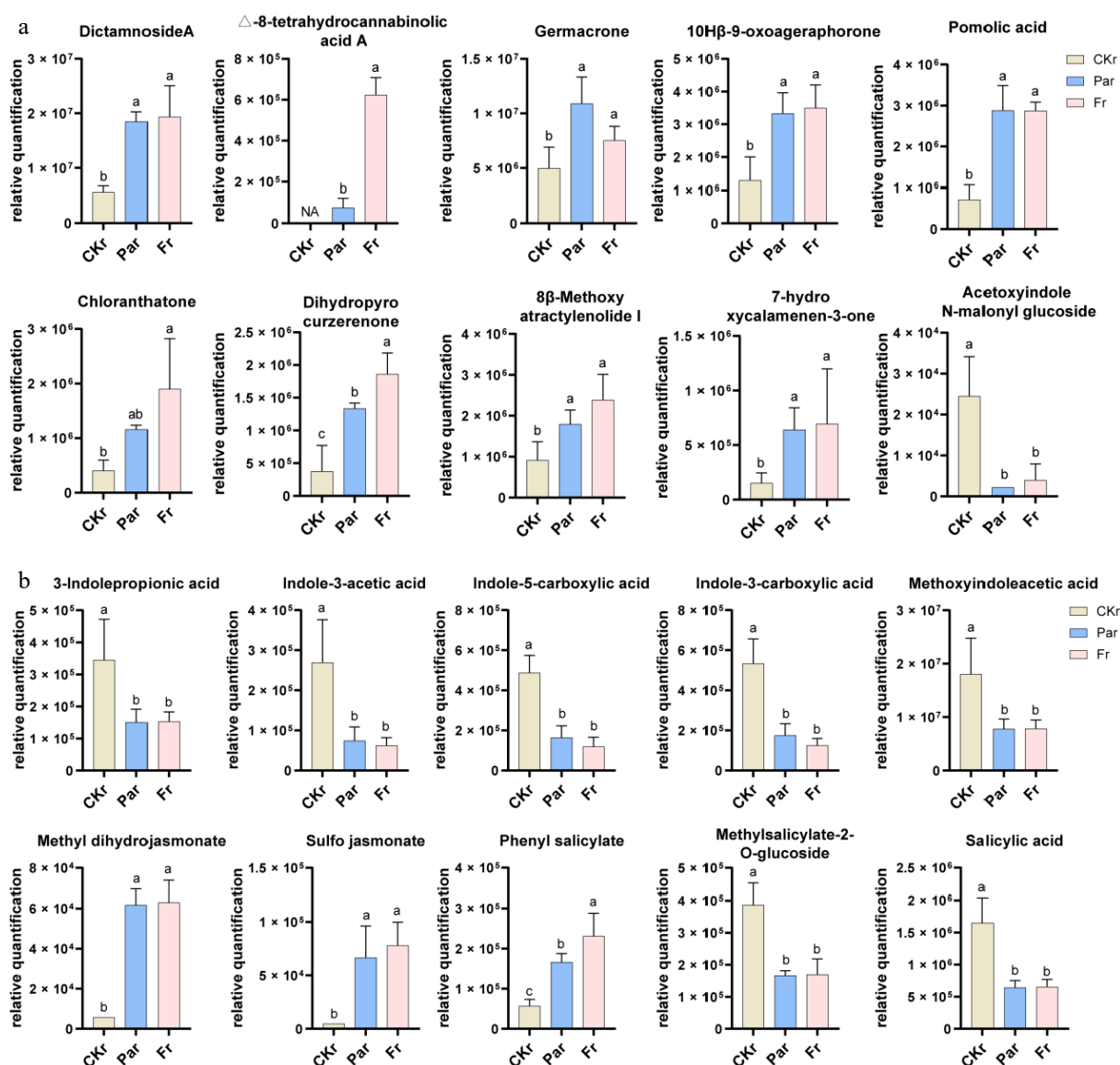
Fig. 3 (a) The bar chart displays the change of the top 10 compounds in content based on differentially accumulated metabolites (DAMs) in *A. lancea* rhizome among the F9 inoculation group, the Pa inoculation group, the free-F9, and the Pa inoculation group. Bar graphs represented as mean ± SEM. The alterations in the levels of plant growth and metabolism-associated hormones, as derived from the DAMs, are quantified and depicted in (b). Different lowercase letters indicate significant differences (one-way ANOVA, $p < 0.05$, $n = 5$).

inoculation led to significant downregulation of the same components, with a minor increase in some compounds.

Among the 271 compounds showing similar changes compared to CKfr post-inoculation with F9 and Pa, 209 compounds were downregulated, while 62 were upregulated. Downregulated compounds were primarily amino acids and derivatives, while upregulated compounds were mostly flavonoids (Fig. 2b). Notably, many compounds exhibited distinct accumulation patterns after F9 and Pa inoculation (Supplementary Fig. S5e–h). Specifically, 86 components were regulated by Pa (Supplementary Fig. S5e), 205 by F9 (Supplementary Fig. S5f), and 101 by F9 or Pa (Supplementary Fig. S5h). F9 inoculation led to a greater upregulation of flavonoids, with 203 compounds compared to Pa's 28 (Fig. 2b). Thus, F9 treatment significantly upregulated flavonoids and downregulated amino acids and derivatives in the fibrous root compared to Pa treatment.

Among flavonoids, the top 10 compounds ranked by peak area were more influenced by F9 than Pa across CKfr, F9fr, and Pafr groups (Fig. 4a). Additionally, the peak areas of nine hormones were

analyzed, revealing that jasmonic acid and sulfo jasmonate displayed similar trends to 11 flavonoids (Fig. 4a and b).

RNA sequencing and transcriptomic assembly

To explore how different compartments in *A. lancea* respond to F9 and Pa at the transcriptional level, 30 cDNA libraries were created from two different compartments (rhizomes and fibrous roots, each with five replicates) of *A. lancea* under three treatments: CK, no inoculation), F9 inoculation, and Pa inoculation. These libraries were sequenced using the NovaSeq platform. The clean reads generated from transcriptome sequencing of the two different compartments of the three groups, after removing polluted adapters, low-quality reads, and reads with a high content of unknown bases (N), are shown in Supplemental Table S6. The mean value of clean reads from every group were 40.52, 41.73, 42.88, 42.15, and 42.33 M, respectively. The Q20 and Q30 values were above 96% and 90%, respectively, and GC contents were between 40% and 50%. The *A. lancea* genome sequence has been completed[20], and the ratio of RNA-seq of every group mapping to the genome sequence was over
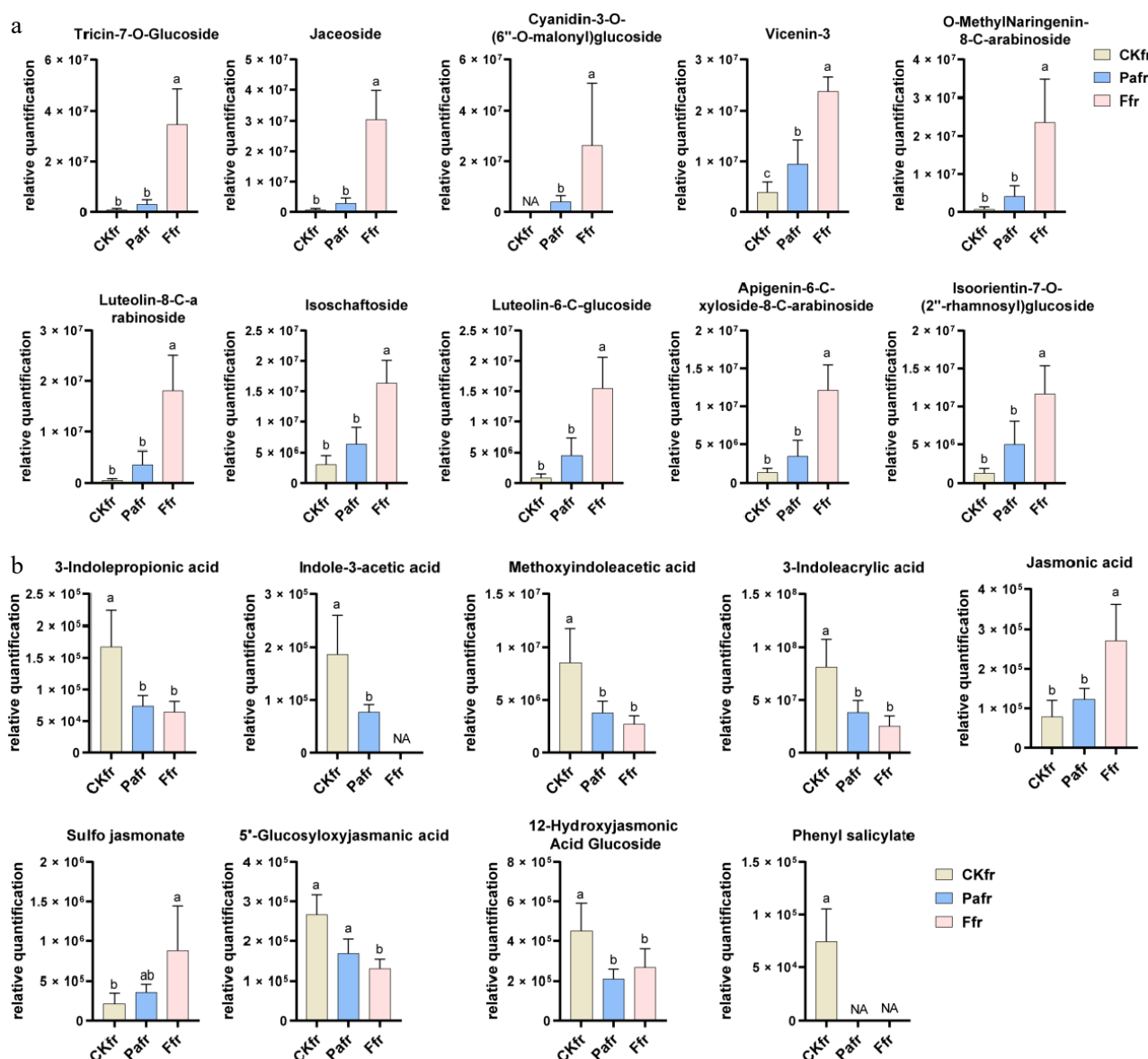
Fig. 4 (a) The bar chart displays the change of the top 11 compounds in content based on differentially accumulated metabolites (DAMs) in *A. lancea* fibrous roots among the F9 inoculation group, the Pa inoculation group, the free-F9, and the Pa inoculation group. Bar graphs represented as mean ± SEM. The alterations in the levels of plant growth and metabolism-associated hormones, as derived from the DAMs, are quantified and depicted in (b). Different lowercase letters indicate significant differences (one-way ANOVA, $p < 0.05$, $n = 5$).

80%. These indices indicated the high quality of the sequencing data. A summary of the transcriptome sequencing data from the rhizome and fibrous root in the three treatments of *A. lancea* are presented in Supplementary Table S6.

Transcriptomic differences in F9 and Pa inoculation treatments in rhizome

To examine if inoculation with F9, Pa, free-F9, and Pa treatments resulted in differences in transcription levels of *A. lancea* rhizomes, PCA analysis was performed on the 15 transcription profiles. The distinct separation in the PCA plot suggested that F9 and Pa inoculation significantly altered the transcriptional programming of *A. lancea* rhizomes (Fig. 5a). Additionally, the transcriptional variations in *A. lancea* induced by F9 (Fr vs CKr) were more prominent than those induced by Pa (Par vs CKr) (Fig. 5b). A total of 5,050 differentially expressed genes (DEGs) were identified from the different pairwise comparison groups (Fr vs CKr, Par vs CKr, Fr vs Par) (Fig. 5b). To

understand the unique effects of F9 and Pa inoculation on *A. lancea* rhizomes, VENN analysis was conducted (Fig. 5c). F9 inoculation resulted in significantly more specific DEGs 2938 (2296 + 642), compared to 390 (340 + 50) in Pa inoculation. Specifically, the number of DEGs after F9 inoculation was 7.5 times greater than those induced by Pa. Thus, F9 inoculation was more likely to cause extensive transcriptional changes in *A. lancea* compared to Pa inoculation. To gain insight into the biological functions of DEGs caused by F9 or Pa inoculation, KEGG enrichment analysis was conducted on these DEGs. Firstly, 166 co-DEGs from Fr vs CKr, and Par vs CKr, and Fr vs Par were analyzed (Fig. 5d). The aim was to elucidate the mechanisms by which *A. lancea* rhizome responded differently to F9 and Pa. Among the top five enriched pathways, there were two sugar-related metabolic pathways and one sesquiterpenoid and triterpenoid biosynthesis. Then, the top five KEGG enrichment results from 1,295 co-DEGs of Fr vs CKr and Par vs CKr, compared to Fr vs Par, included linoleic acid metabolism, flavonoids and flavonol
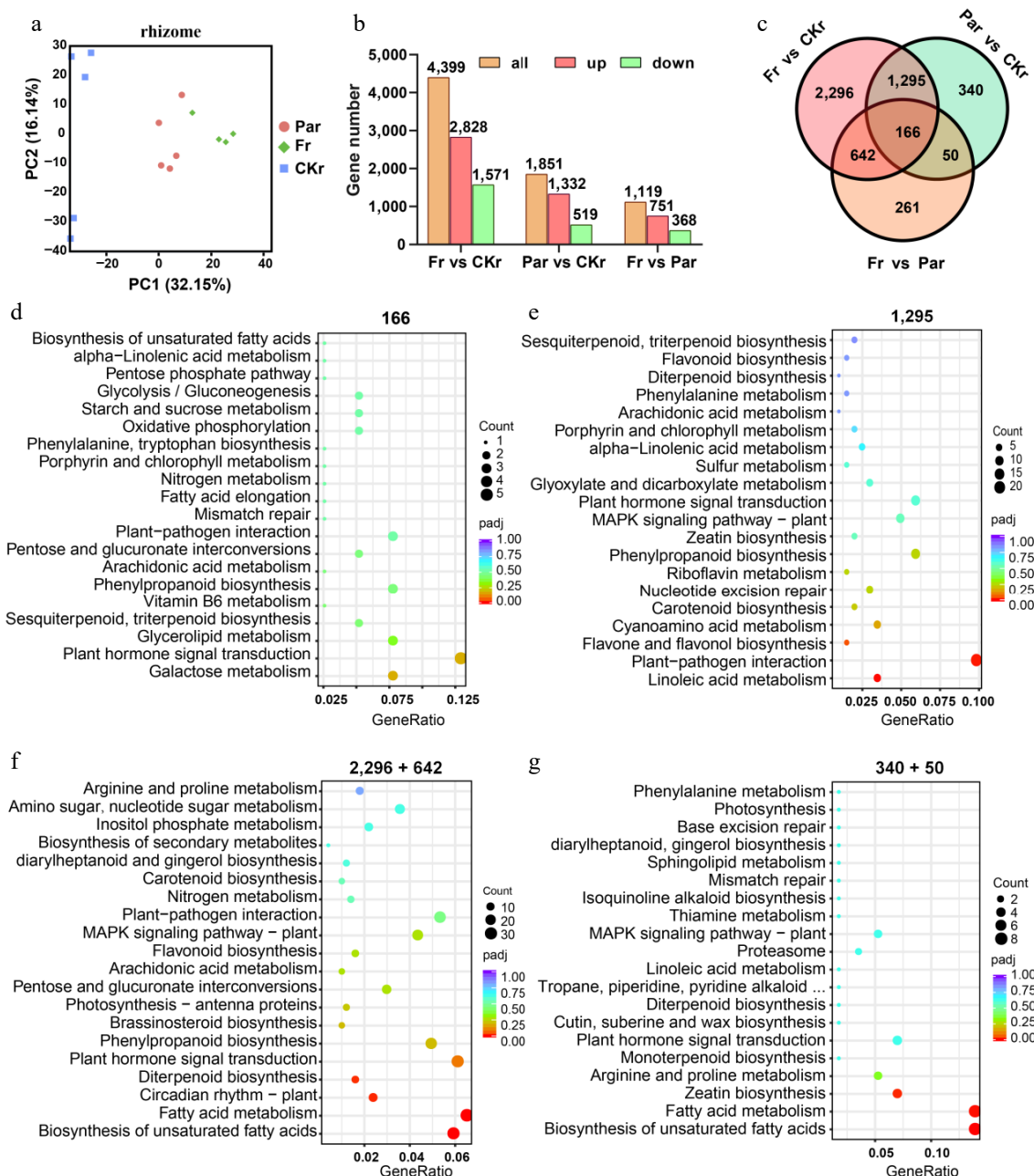
Fig. 5 Differentially expressed genes (DEGs) and Kyoto Encyclopedia of Genes and Genomes (KEGG) pathway enrichment analysis of transcriptional levels in *A. lancea* rhizome following F9 and Pa inoculation. (a) Principal component analysis (PCA) based on transcriptional data from samples treated with F9 inoculation (Fr), Pa inoculation (Par), or without inoculation (CKr). (b) Statistical analysis of DEGs ($p < 0.05$, |Log$_2$Foldchange| > 1) comparing Fr vs CKr, Par vs CKr, and Fr vs Par, revealing a total of 5,050 DEGs. (c) Venn diagram classifying DEGs into seven groups based on their expression levels across the three treatment conditions. (d)–(g) KEGG pathway enrichment analysis was performed on six of the seven categories, including 1,295, 166, 2,296 and 642, 340 and 50. The 1,295 genes showed similar expression levels between the F9 and Pa inoculation groups; 166 genes exhibit significant differences in expression between these two groups; 2,296 and 642 genes are specifically affected by F9 but not by Pa inoculation; 340 and 50 genes are specifically affected by Pa but not by F9 inoculation.

biosynthesis, plant-pathogen interactions, and carotenoids biosynthesis (Fig. 5e). From the 2296 + 642 DEG group, the KEGG result showed that F9-specific pathways included circadian rhythm, and photosynthetic antenna proteins (Fig. 5f). Notably, compared to Pa induction, F9 had a certain regulatory effect on the light signal transduction and photosynthesis system of *A. lancea* rhizomes.

In this study, the top 20 pathways from the KEGG pathway analysis of each DEGs region were investigated. The genes involved in 23 metabolic pathways were summarized, including the photosynthesis system, sugar metabolism pathway, hormone pathway, upstream pathway of hormone biosynthesis, flavonoids, sesquiterpenes, and

the unsaturated fatty acid pathway. Correlation analysis was conducted with these pathways and related terpenoids with reported biological activity (GM, PA, AYC, CZT, CZC, CZS, Me_O_atelide), and phytohormones (IAA, MeSA-Glu, 2H_MeJA) (Fig. 6a). IAA and MeSA_Glu showed negative correlations with active ingredients, while 2H_MeJA showed statistically significant positive correlations. To identify potential key genes regulating active ingredients, matrix correlation analysis was performed on 23 pathways obtained from KEGG enrichment results with AYC affected by F9 and Pa differences, and CZT not affected by F9 and Pa differences. Compared to 14 pathways related to AYC, 80 genes with a
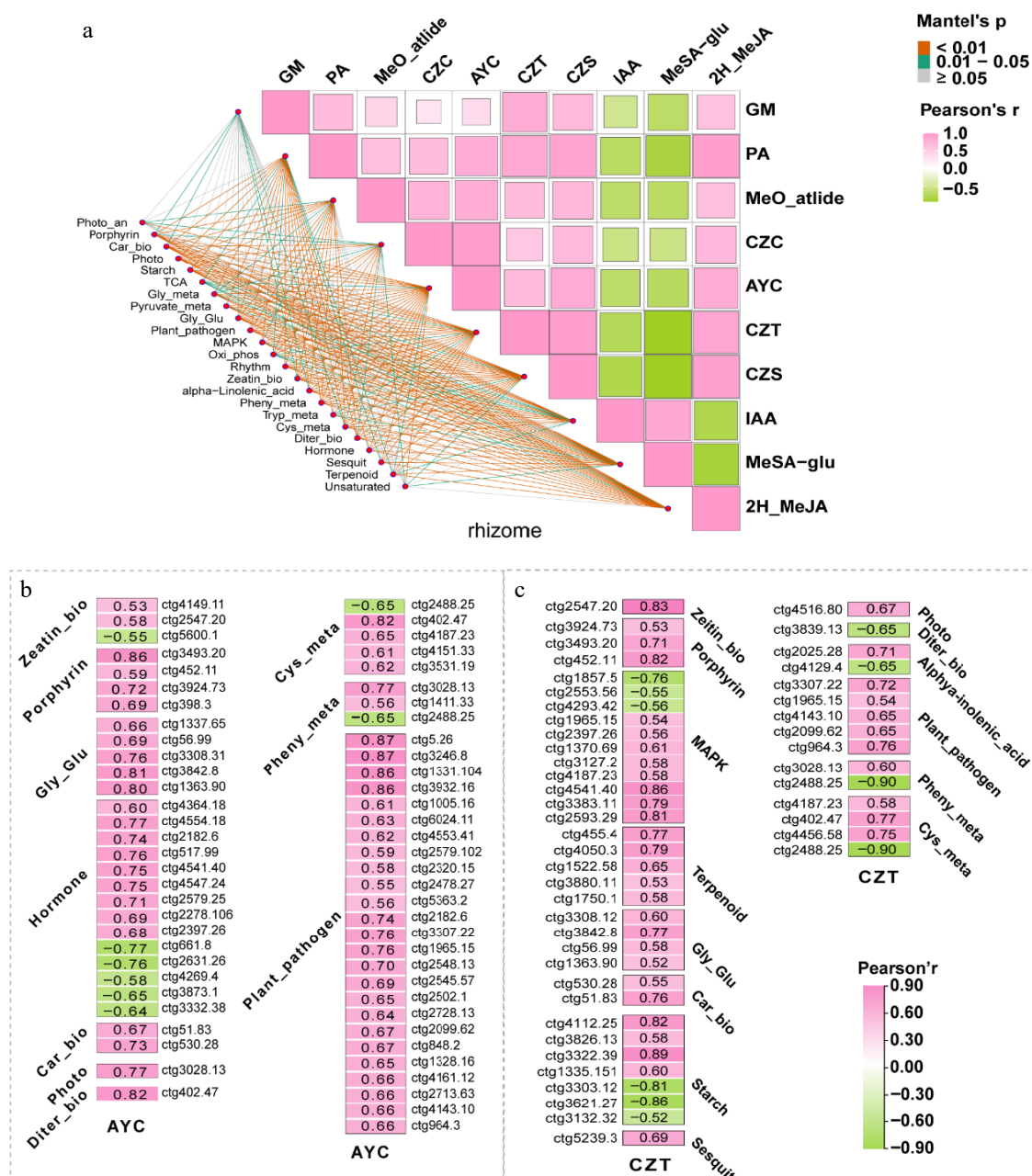
Fig. 6 (a) Matrix correlation analysis between traits, including metabolites and growth phenotypes, in response to F9 and Pa inoculation, and the KEGG enrichment pathway in *A. lancea* rhizome. (b) Pearson correlation analysis was also performed between two medicinal terpenoids (AYC and CZT) and the genes within the screened KEGG enrichment pathway in the rhizome of *A. lancea*. Abbreviation: GM: Germacrone; PA: Pomolic acid; CZC: Hinesol; AYC: *β*-eudesmol; CZT: Atractylon; CZS: Atractylodin; IAA: Indole-3-acetic acid; MeSA-glu: Methylsalicylate-2-O-glucoside; 2H_MeJA: Methyl dihydrojasmonate. Zeatin_bio: Zeatin biosynthesis, Porphyrin: Porphyrin and chlorophyll metabolism, Gly_Glu: Glycolysis/Gluconeogenesis, Hormone: Plant hormone signal transduction, Car_bio: Carotenoids biosynthesis, Photo: Photosynthesis, Diter_bio: Diterpenoid biosynthesis, Cys_meta: Cysteine and methionine metabolism, Plant-pathogen: Plant-pathogen interaction, MAPK: MAPK signaling pathway, Terpenoid: Terpenoid backbone biosynthesis, Pheny_bio: Phenylpropanoid biosynthesis, Starch: Starch and sucrose metabolism, Sesquit: Sesquiterpenoid and triterpenoid biosynthesis, Alpha-Linolenic_acid: alpha-Linolenic acid metabolism.

correlation coefficient of |r| > 0.5 were screened (Fig. 6b). Similarly, 15 pathways related to CZT were analyzed, and 51 genes with a correlation coefficient of |r| > 0.5 were screened (Fig. 6c). The DEGs obtained through screening were annotated based on the genome and are shown in Supplementary Table S7.

Transcriptomic differences in F9 and Pa inoculation treatments in fibrous root

The PCA plot's clear separation degree suggests that F9 and Pa inoculation significantly alter the transcriptional programming of

A. lancea fibrous root (Fig. 7a). Transcriptional variations in *A. lancea* induced by F9 (Ffr vs CKfr) are more prominent than those induced by Pa (Pafr vs CKfr) (Fig. 7b). Both F9 and Pa inoculation result in a higher number of upregulated genes than downregulated genes (Fig. 7b). A total of 6,627 DEGs were obtained from the different pairwise comparison groups (Ffr vs CKfr, Pafr vs CKfr, Ffr vs Pafr) (Fig. 7b). To comprehend the distinct effects of F9 and Pa inoculation on *A. lancea* fibrous roots, Venn analysis was performed on each differential region (Fig. 7c). The specific DEGs in the transcriptional
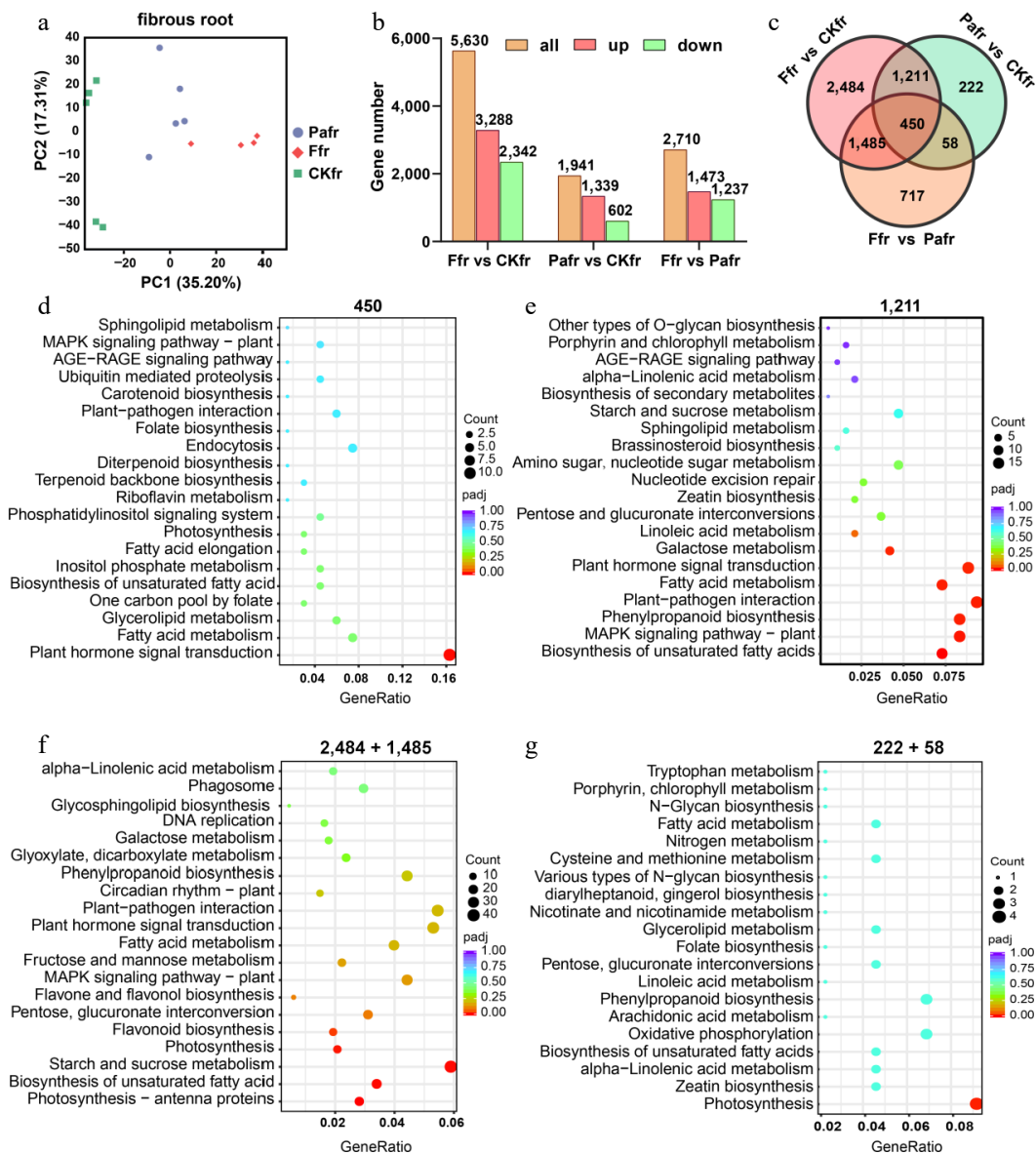
Fig. 7 Differentially expressed genes (DEGs) and enrichment analysis of Kyoto Encyclopedia of Genes and Genomes (KEGG) pathways in *A. lancea* fibrous roots affected by F9 and Pa inoculation. (a) Principal component analysis (PCA) of transcriptional data from samples treated with F9 inoculation (Ffr), Pa inoculation (Pafr), and without inoculation (CKfr). (b) Statistical analysis of DEGs ($p < 0.05$, |Log$_2$Foldchange| > 1) from comparisons of Fr vs CKfr, Pafr vs CKfr, and Ffr vs Pafr, identifying a total of 6,627 DEGs. (c) Venn diagram classifying DEGs into seven groups based on their expression patterns across the three treatments. (d)–(g) Kyoto Encyclopedia of Genes and Genomes (KEGG) pathway enrichment analysis was performed on six of the seven categories, representing 1,211, 450, 2,484 and 1,485, 222, and 58 DEGs. The 1,211 DEGs show similar expression levels between the F9 and Pa inoculation groups; 450 DEGs show significant differences between these groups; 2,484 and 1,485 DEGs are specifically affected by F9 but not by Pa inoculation; 222 and 58 DEGs are specifically affected by Pa but not by F9 inoculation.

profile of *A. lancea* fibrous root following F9 inoculation are significantly higher, with 2484 DEGs identified, compared to the 222 specific DEGs observed following Pa inoculation. Specifically, the number of DEGs in the transcriptional profile of fibrous root after F9 inoculation is 11.1 times greater than that induced by Pa. Consequently, F9 inoculation is more likely to cause extensive transcriptional changes in *A. lancea* fibrous root compared to Pa inoculation. To gain a deeper understanding of the biological functions of DEGs in fibrous root treated with F9 or Pa, KEGG enrichment analysis was conducted on these DEGs (Fig. 7d–g). Firstly, KEGG analysis was conducted on 450 co-DEGs from Ffr vs CKfr and Pafr vs CKfr, as well as Ffr vs Pafr, which represent the differences in fibrous root responses to F9 and Pa. The top five enriched pathways included plant hormone signal transduction, fatty acid metabolism, and the

biosynthesis of unsaturated fatty acids (Fig. 7d). Subsequently, KEGG enrichment results for 1,211 co-DEGs from Ffr vs CKfr and Pafr vs CKfr, excluding Ffr vs Pafr, which represent the similarities in fibrous root responses to F9 and Pa, revealed that the top five enriched pathways were biosynthesis of unsaturated fatty acid, MAPK-signaling pathway-plant, phenylpropanoid biosynthesis, plant-pathogen interaction, and fatty acid metabolism, followed by plant hormone signal transduction (Fig. 7e). Lastly, KEGG analysis of 3,969 (2,484 + 1,485) co-DEGs in response to F9 but not Pa revealed that F9 significantly induced changes in photosynthesis-antenna pathway related genes, biosynthesis of unsaturated fatty acid, starch and sucrose metabolism, photosynthesis, and flavonoid and flavonoid biosynthesis pathways in *A. lancea* fibrous root, while Pa significantly induced changes in photosynthesis-related genes.

A summary of KEGG pathways was conducted using the same method and criteria as for rhizomes. A total of 24 pathways were used for analysis. Matrix correlation analysis was conducted on these pathways with related indices, including flavonoids with reported biological activity (TR (Tricin-7-O-Glucoside), VI [Vicenin-3]), phytohormones (IAA, JA), medicinal compounds (CAC, CZT), and growth indices (FW, RL) (Fig. 8a). Firstly, the correlation between each index was observed (Fig. 8a). IAA showed a negative correla-

tion with root growth and four metabolic compounds (TR, VI, CZC, CZT), while JA and flavonoids (TR, VI), growth indices (FW, RL) exhibited a significant positive correlation. Additionally, the correlation coefficient between the two flavonoid components and the two terpenoid components was relatively small.

To compare the differential effects of F9 and Pa on the transcription level of *A. lancea*, matrix correlation analysis was performed on 24 pathways obtained from KEGG with TR affected by F9 and Pa
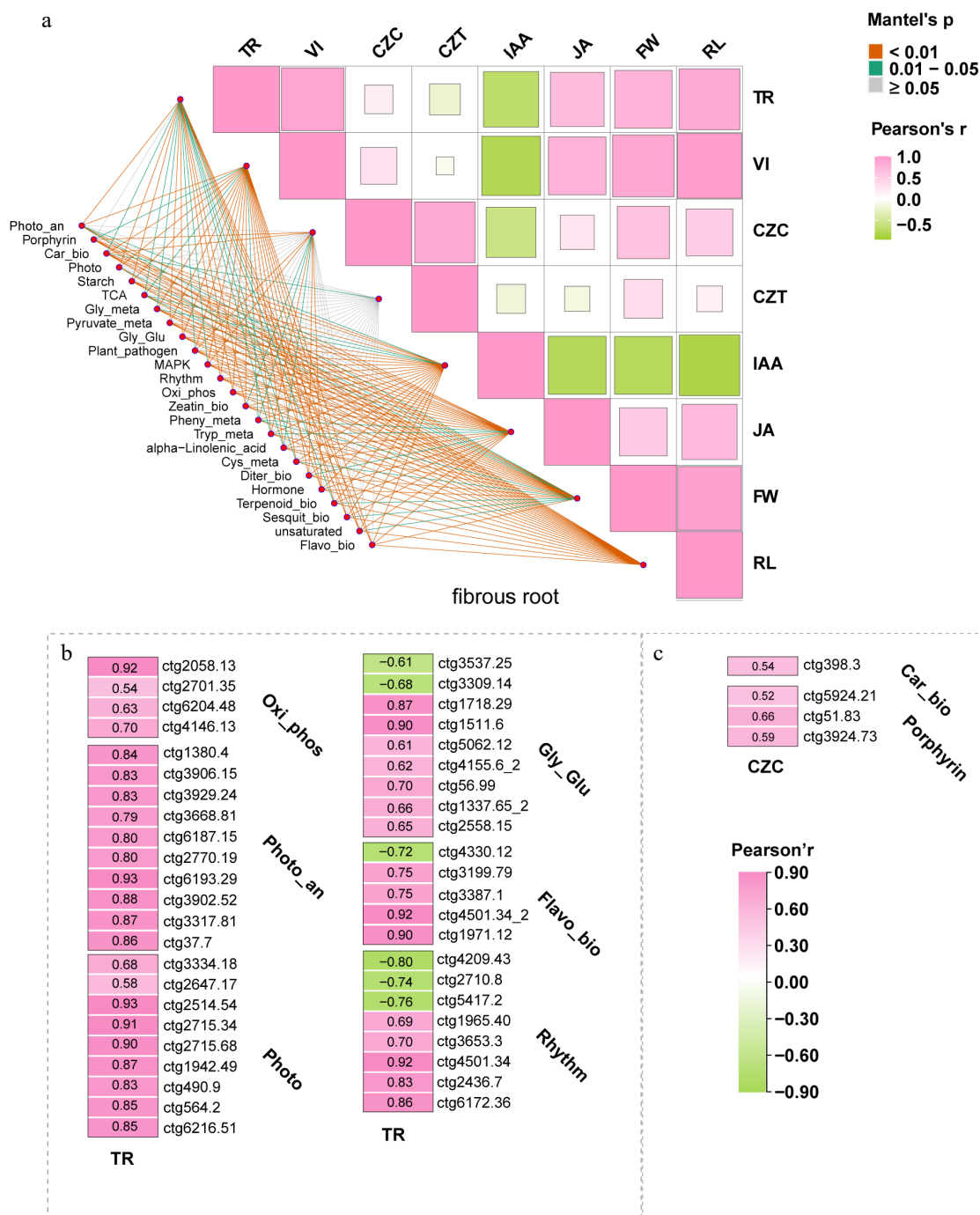

Fig. 8 (a) Matrix correlation analysis between traits, including metabolites and growth phenotypes, in response to F9 and Pa inoculation, and the KEGG enrichment pathway in *A. lancea* fibrous roots. (b) Pearson correlation analysis was also performed between two key metabolites (TR and CZC) and the genes within the screened KEGG enrichment pathway in the fibrous roots of *A. lancea*. Abbreviation: TR: Tricin-7-O-Glucoside; VI: Vicenin-3; CZC: Hinesol; CZT: Atractylon; IAA: Indole-3-acetic acid; JA: Jasmonic acid; FW: fresh weight of the whole plant; RL: root lengths; Oxi_phos: Oxidative phosphorylation; Photo-an: Photosynthesis-antenna proteins; Photo: Photosynthesis; Gly_Glu: Glycolysis/Gluconeogenesis; Flavo_bio: Flavonoid biosynthesis; Rhythm: Circadian rhythm-plant; Car_bio: Carotenoids biosynthesis; Porphyrin: Porphyrin and chlorophyll metabolism.

differences, and CZC not affected by F9 and Pa differences. Six pathways related to TR were obtained, and further Pearson correlation analysis (Fig. 8b) was performed to screen for 45 genes with |r| > 0.5. Four pathways related to CZC were obtained, and further Pearson correlation analysis was performed to screen for four genes with an |r| > 0.5 (Fig. 8c). The DEGs obtained through screening were annotated based on the genome (see Supplementary Table S7).

Mining for terpene and flavonoid accumulation's regulator TFs in *A. lancea*

Based on the transcriptome analysis of the 5,050 DEGs from the rhizome, 327 transcription factors from 36 transcription factor families were identified. From the top 15 transcription factor families, 264 genes were selected for further analysis. A correlation analysis was conducted between these genes and six components: CZS, CZT, CZC, AYC, Methyl dihydrojasmonate (2H_MeJA), Indole-3-acetic acidx (IAA), Methyl Salicylate Oxygenate (MeSA_glu), Pomolic acid (PA), and Germacrone (GM). Genes with a correlation coefficient |r| ≥

0.8 and *p* < 0.05 were considered significantly correlated. This analysis screened out 41 transcription factors, of which 18 were significantly positively correlated with indoleacetic acid and methyl salicylate glycoside, and 49 were positively correlated with other components (Fig. 9b).

Similarly, from the fibrous root's 6,628 DEGs, 432 transcription factors from 36 transcription factor families were identified. From the top 15 transcription factor families, 338 genes were selected for further analysis (Fig. 9c). A correlation analysis was conducted between these genes and six components: CZT, CZC, FW, TR, RL, VI, JA, and IAA. Genes with a correlation coefficient |r| ≥ 0.8 and a *p*-value < 0.05 were considered significantly correlated, resulting in 65 transcription factor genes (Fig. 9d).

RT-qPCR verification

The expression of genes involved in plant hormone signal transduction, MAPK signaling pathway, plant-pathogen interaction, and sesquiterpenes and triterpenes biosynthesis pathway was
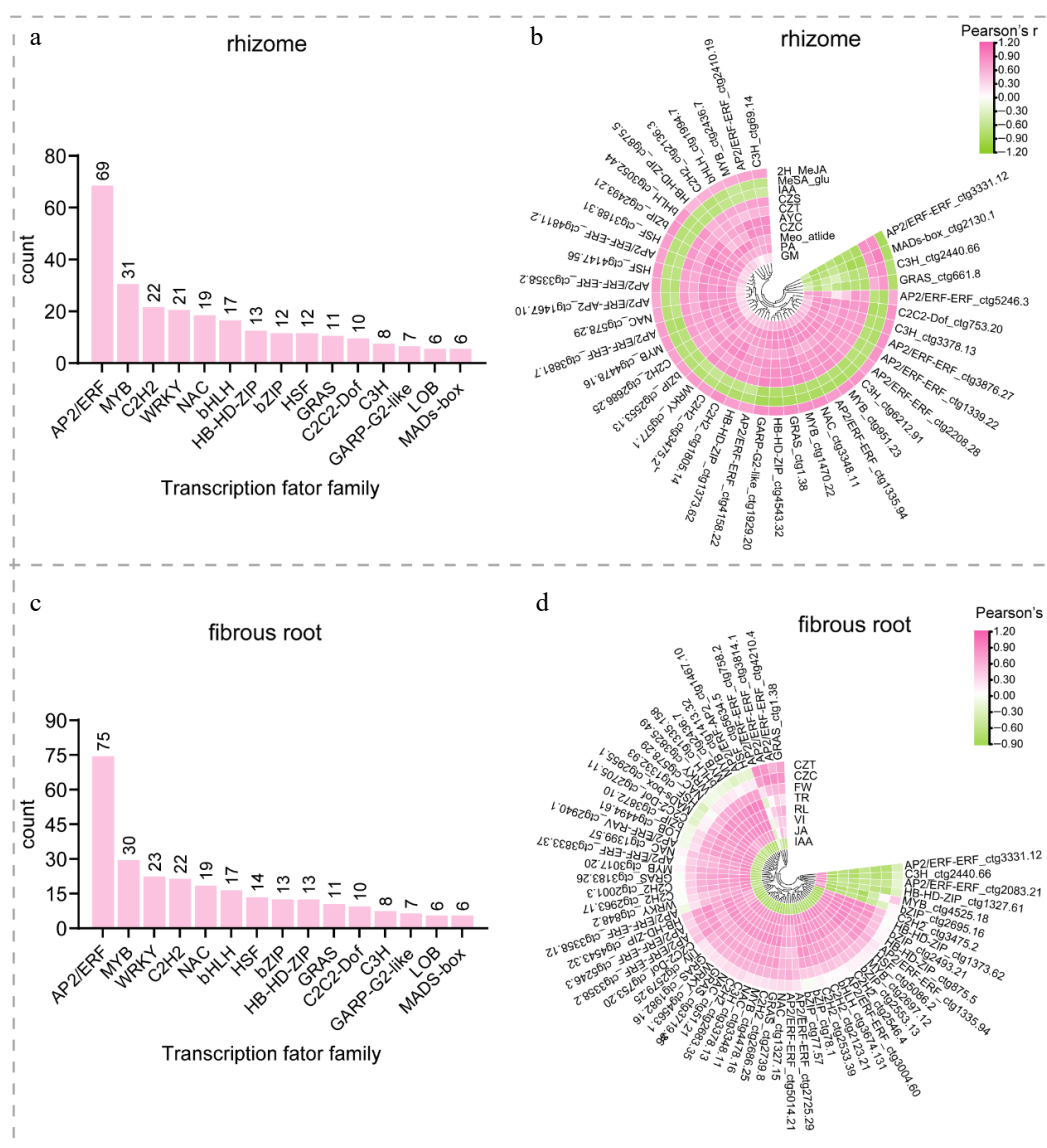

Fig. 9 (a) The different transcription families based on the number of transcriptional regulatory genes from differentially expressed genes (from high to low). The number of transcription factors in each family was recorded. (b) Correlation analysis was performed between traits and the express level of transcriptional factors. 2H_MeJA: Methyl dihydrojasmonate; GM: Germacrone; CZC: Hinesol; AYC: *β*-eudesmol; CZT: Atractylon; CZS: Atractylodin; IAA: Indole-3-acetic acid; MeSA_glu: Methylsalicylate-2-O-glucoside; PA: Pomolic acid; FW: fresh weight of the whole plant; RL: root lengths; TR: Tricin-7-O-Glucoside; RL: root lengths; VI: Vicenin-3; JA: Jasmonic acid.

significantly activated in F9 or Pa inoculation. Based on the correlation analysis between the obtained components and genes, genes positively correlated with the main active components were selected for quantitative real-time reverse transcription polymerase chain reaction (RT-qPCR) verification (Supplementary Fig. S6). The results were consistent with the expression trend of each gene in the transcriptome, indicating that the transcriptome sequencing from which the gene expression was obtained was relatively accurate.

Discussion

Both the endophytic fungus F9 and the endophytic bacteria Pa significantly promoted the growth and active compound accumulation of *A. lancea*, as evidenced by increased fresh weight of the underground compartment, enhanced fibrous root elongation, and elevated accumulation of hinesol, β-eudesmol, atractylon, and atractylodin. Yuan also reported that endophytic fungus AL12 markedly promoted both biomass accumulation and terpenoid biosynthesis in *A. lancea*[29]. Collectively, these findings provide a foundation for integrating beneficial microbial consortia into field cultivation strategies to improve the yield and quality of *A. lancea*. From a growth perspective (Fig. 1a–g), fungus F9 had a better growth-promoting effect than bacterium Pa. The chlorophyll a/b ratio is an indicator of a plant's efficiency in absorbing and utilizing light energy. A higher ratio indicates increased light energy capture and enhanced photosynthetic activity[30]. Figure 1g showed the improvement in photosynthetic activity in *A. lancea* by F9 inoculation. At the transcriptional level, the present analysis reveals a significant positive correlation between the flavonoid glycoside TR content in fibrous roots, and the expression of genes associated with photosynthesis-related pathways (Fig. 8b). Given the significant positive correlation observed between fresh weight (Fig. 1b) and flavonoid glycoside TR, the expression of genes associated with photosynthesis-related pathways is positively correlated with the fresh weight. In addition, it has been demonstrated that fungi have a promoting effect on *A. lancea* in enhancing plant photosynthesis compared to bacteria. Pandey et al.[31] demonstrated that inoculation with 11 endophytic fungi and 32 endophytic bacteria isolated from *Withania somnifera* plants improved the photosynthetic efficiency of *W. somnifera* compared to non-inoculated control plants. However, endophytic bacteria did not significantly improve the measured photosynthesis. Hou et al.[32] further showed that the inoculation of soil microbes at the plant root can enhance the crown width of aboveground leaves and alleviate low light stress. In summary, compared to endophytic bacteria Pa, endophytic fungus F9 significantly enhances the *A. lancea* photosynthetic efficiency and facilitates the accumulation of primary metabolites, thereby increasing its biomass. Consequently, this improved photosynthetic activity ensures a sustained supply of carbon resources in the root, which is essential for the survival and maintenance of the associated fungi. Future research on how fungi boost plant photosynthesis is a valuable topic that will enhance our understanding of the ecological roles of functional strains in plants. Studies have shown that *Pseudomonas fluorescent* ALEB7B from *A. lancea* inhibited the southern blight of *A. lancea*[33]. However, the present study did not assess the inhibitory effects of endophytes on pathogenic bacteria. Therefore, besides research aimed at enhancing the growth and quality of *A. lancea*, there is scope for investigating the mitigation of continuous cropping obstacles, soil-borne diseases, and other related challenges through endophyte application.

Comparative metabolomics of *A. lancea* rhizomes revealed that terpenoids were the most significantly enriched class upon endophyte inoculation (Fig. 2a). Further, it was found that the accumulation of most terpenoids, including the sesquiterpene atractylon, was independent of endophytic strain types. By contrast, a limited number of compounds, such as the sesquiterpenes hinesol and β-eudesmol, exhibited differential responses to the change of endophytic strain types (Fig. 1h, i). This finding suggested that these compounds are unsuitable as an evaluation metric for future strain selection or optimization in the construction of *synthetic microbial consortia*. Furthermore, Pearson correlation analysis revealed a statistically significant positive association between the content of atractylon, β-eudesmol, and the expression of the immunity pathway-related genes in *A. lancea*, including plant-pathogen interaction, plant hormone signaling, and the MAPK signaling pathway (Fig. 6b). The primary regulation of terpenoids by F9 or Pa in the rhizome was likely due to their defensive function in inhibiting microbial overgrowth and mitigating its detrimental effects. *A. lancea*, a perennial root herb, relies on its rhizome, a key compartment, to prolong its vitality and survive the cold winter season. Terpenes, the compounds with aromatic and volatile odors, may play a defensive role in driving away soil pests and pathogens or attracting their natural enemies to protect the growth of the rhizome. Numerous studies have demonstrated the role of terpenes in insecticidal, bactericidal, and weed control, and they have been developed as botanical pesticides[34]. The significant positive correlation was observed between atractylon and the jasmonic acid derivative 2H-MeJA. Jasmonate was a pivotal hormonal signal during plant immunity. Ren & Dai[35] have previously demonstrated that jasmonate mediated endophyte-induced biosynthesis of sesquiterpenoids in *A. lancea*. Consequently, the preliminary results indicated that upon perception of endophytic fungus F9, *A. lancea* activated the jasmonate-dependent terpenoid biosynthetic pathway, thereby reinforcing its immune defence. Further transcriptome-level analysis revealed the immunity mechanisms mediated by terpenoids in *A. lancea* rhizomes in response to endophyte infection (Fig. 6b, c). We identified genes significantly positively correlated ($p < 0.05$) with terpenoids AYC, which were differentially influenced by F9 and Pa inoculation, and genes associated with CZT, which were similarly affected by F9 and Pa inoculation (Figs 6b, 9a). These genes were annotated as *CNGC*, *CAM*, *CPK*, *MPK*, *MKK*, *TIFFY*, *MYC2*, and *WRKY* (Supplementary Table S7) in immunity-related pathways (Figs 6b, c, 9a). Ren & Dai found that Ca^{2+} dependent protein kinase (CPK) activities were required for endophyte-induced terpenoid production in *A. lancea* plantlets using pharmacological and biochemical approaches[36]. The activation of CPKs and MPKs phosphorylates a specific WRKY transcription factor subgroup to respond to plant growth and metabolic regulation by microorganisms[37−39]. Hao et al. demonstrated an interaction between WRKYs-MYC2 in regulating secondary metabolism in plants[40]. Additionally, the terpenoid synthesis regulation by WRKY and MYC2 family transcription factors has been proven by numerous studies[41,42]. In summary, the mechanism through which fungus and bacteria stimulate terpenoid synthesis may involve the activation of *A. lancea* rhizome cells, leading to Ca^{2+} influx. Ca^{2+} then acts as a secondary signal to initiate a cascade reaction involving CNGC, CAM, CPK, MPK, and MKK protein kinases, which promote the binding of transcription factors (MYC2 and WRKYs) of immunity pathways with key enzyme genes of sesquiterpenes biosynthesis. The regulatory mechanisms underlying endophyte-induced sesquiterpenoid accumulation revealed in our study diverge from those reported by Yuan et al[29]. Whereas Yuan et al. observed a

predominant down-regulation of immunity-related genes in *A. lancea* following inoculation with the endophytic fungus AL12, our results demonstrate a marked up-regulation of genes implicated in immune pathways after inoculation with the endophytic fungus F9. A comparative evaluation of the experimental methodologies reveals that Yuan[29] derived their immune-response data from aerial leaf tissues, whereas the present study examined the rhizome and fibrous roots. Therefore, the observed opposite immune responses may be attributed to the fact that the immune responses of aerial and underground tissues of *A. lancea* to endophytic fungi exhibit tissue specificity.

In *A. lancea* fibrous root, metabolomic analysis revealed that flavonoids, rather than terpenoids, were the predominant class of upregulated compounds (Fig. 2b), which aligned with previous research findings. The upregulated flavonoids primarily consisted of flavonoid glycosides and isoflavone glycosides, with aglycone structures including tricin, naringenin, quercetin, luteolin, and apigenin, among others (Fig. 4a). Flavonoids have been extensively studied due to their role in plant-microbe interactions[43]. Early *in vitro* studies suggested that flavonoids induce the expression of the rhizobia nod gene. For instance, alfalfa (*Medicago sativa*) seed imbibition leads to the accumulation of quercetin-3-O-galactoside (a flavonol) and luteolin-7-O-glucoside (a flavone), enhancing the growth rate of *Rhizobium meliloti*[44]. Flavonoid-deficient roots had a near complete loss of nodulation by *Sinorhizobium meliloti*, whereas flavone-deficient roots have reduced nodulation[45]. Consequently, upregulated flavonoids (tricin-7-O-Glucoside, luteolin-8-C-arabinoside) serve a

communicative function in facilitating the colonization of endophytic fungi and bacteria. Oxidative phosphorylation is a critical energy conversion mechanism in plants, with photosynthesis serving as the primary energy supplying physiological process. Energy and carbon sources are transferred as glycosides, which comprise flavonoids and sugars in fibrous root. A significant positive correlation has been observed between flavonoid transfer rates (TR) and oxidative phosphorylation and photosynthesis pathway-related genes, thereby suggesting that upregulated flavonoids may function as energy sources for microorganisms during plant-microbe interactions. Jasmonic acid is a hormone known to respond to plant immunity[35]. The positive correlation observed between flavonoid glycoside TR and jasmonic acid suggests that flavonoid glycoside compounds may also contribute to the defensive mechanisms in roots. In summary, flavonoids play multiple roles in fibrous roots, including promoting colonization, defense, and energy supply. Fungal endophyte F9 and bacterial endophyte Pa both facilitated the accumulation of flavonoids and their derivatives in the fibrous roots of *A. lancea*, showing comparable promotive effects. However, a more pronounced response to F9 was observed in the accumulation of substantial quantities of flavonoids compared to Pa (Fig. 2b). For example, Begum et al. found that Arbuscular Mycorrhizal Fungus (AMF) significantly increased flavonoids in tobacco plants compared to Rhizosphere bacteria (PGPR)[46]. Flavonoids can have beneficial effects on specific bacterial communities. The soil treated with daidzein increased the relative abundance of *Comamonadaceae*[47], while the quercetin treatment resulted in a
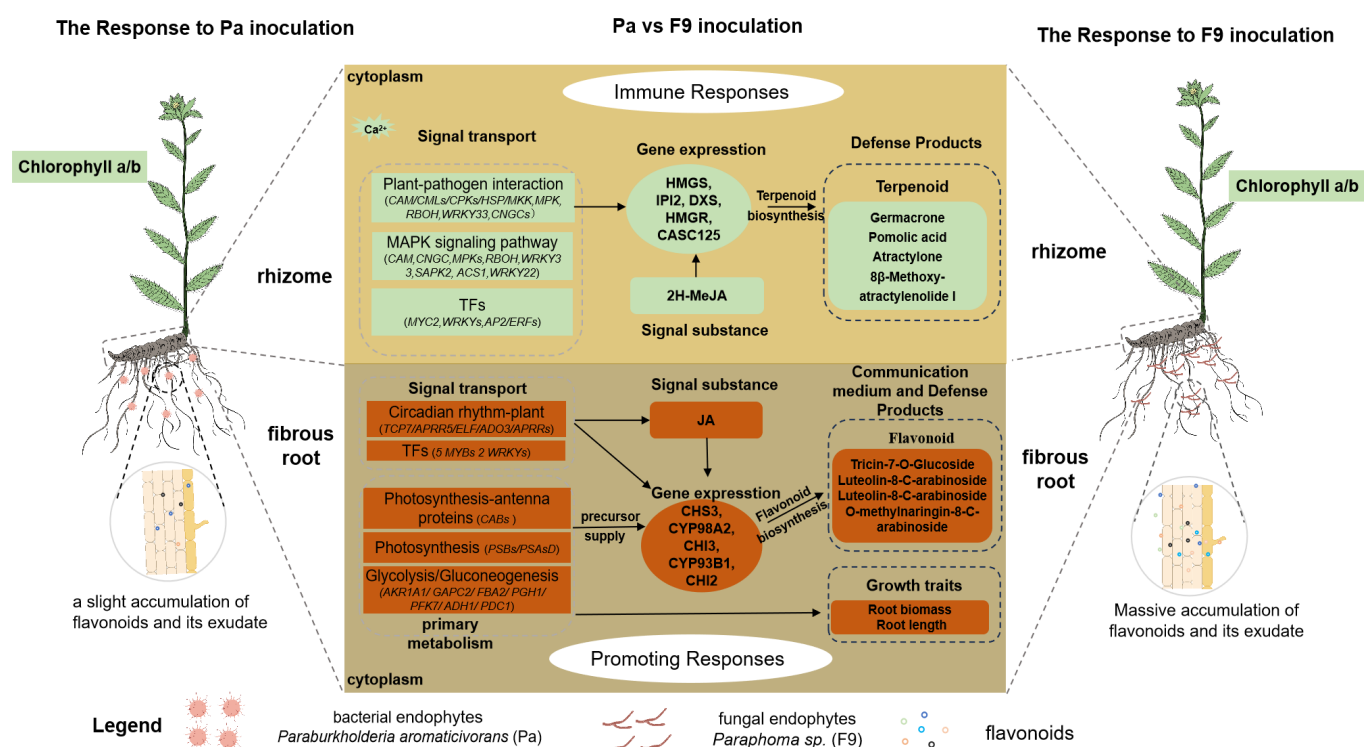

Fig. 10 Simplified schematic summary of the differential mechanisms promoting host growth and metabolism in *A. lancea* at the transcriptional level in response to the endophytic fungus *Paraphoma sp.* (F9) and the endophytic bacterium *Paraburkholderia aromaticivorans* (Pa). The white oval box represents the primary transcriptional responses, including immune and growth-promoting responses, following endophyte inoculation. The mint green box highlights a significant increase in immune response and terpenoid production in *A. lancea* rhizomes after inoculation with F9 or Pa, compared to the control (F9-free and Pa-free inoculation). However, the magnitude of the immune response is similar between the F9 and Pa treatments. The brownish-red box indicates that F9 inoculation leads to stronger signal transduction, primary metabolism, gene expression, flavonoid accumulation, and overall growth compared to Pa inoculation. The black solid arrow represents promotion. TFs: transcription factors, JA: jasmonic acid, 2H_MeJA: methyl dihydrojasmonate.

relative enrichment of *Pseudarthrobacter* and a higher overall relative abundance of *Proteobacteria*[48]. Additionally, flavone compounds, such as apigenin and luteolin, reportedly enhanced the abundance of *Oxalobacteraceae* in the plant rhizosphere[49]. Specific flavonoid glycosides (tricin-7-O-Glucoside, luteolin-8-C-arabinoside) exhibited significant accumulation when stimulated by F9, rather than Pa, suggesting that flavonoid glycosides may serve as specific signaling molecules that facilitate the recruitment of fungal F9. Based on correlation analysis (Figs 8b, 9d), the significant accumulation of flavonoids is not only linked to the enhanced synthesis of primary metabolites driven by photosynthesis but also highlights its complex relationship with transcriptional regulation. Numerous studies have demonstrated that flavonoids were regulated by multiple transcription factors from the MYBs and WRKYs families[50]. Specifically, five *MYBs* (*MYB_ctg4478.16*, *MYB_ctg2436.7*, *MYB_ctg1413.32*, *MYB_ctg2697.12*, and *MYB_ctg3017.20*), and three WRKYs (*WRKY_ctg848.2*, *WRKY_ctg4563.1*, and *WRKY_ctg3825.49*) contribute to the acceleration of flavonoid biosynthesis (tricin-7-O-Glucoside, luteolin-6-C-glucoside, and luteolin-8-C-arabinoside) by directly regulating the flavonoid biosynthetic genes *CHS3*, *CHIs*, *CYP93B1*, and *CYP98A2*. Further investigation is necessary to elucidate the crucial role of flavonoids, particularly compounds with high content such as tricin-7-O-Glucoside, luteolin-6-C-glucoside, luteolin-8-C-arabinoside, and O-MethylNaringenin-8-C-arabinoside, in the plant-microbe interaction process within the root system.

Conclusions

This study systematically investigated the differential regulatory effects of endophytic fungus F9, and endophytic bacterium Pa on the growth and secondary metabolite accumulation of *A. lancea*. The core findings indicated that fungus F9 exhibited stronger advantages in promoting biomass accumulation and root development due to its ability to boost photosynthesis at the transcriptional level and improve chlorophyll functionality. However, the two have similar effects in promoting the accumulation of terpenoids in rhizomes. The current study has preliminarily revealed the potential molecular mechanism by which endophytes regulate key transcription factors such as MYC2 and WRKYs to enhance terpene biosynthesis by triggering Ca^{2+} signaling flow and kinase cascade reactions (CNGC/CAM/CPK/MPK/MKK). In addition, fungus F9 specifically and significantly activated the biosynthesis of flavonoid compounds in *A. lancea fibrous roots*, such as triterpen-7-O-glucoside, luteolin-6-C-glucoside, lutein-8-C-arabioside, and O-methyl-naringin-8-C-arabinoside compared to bacteria Pa. These flavonoids may be the specific key mediators involved in the interaction between *A. lancea* and endophytic fungus F9. However, this activation may be related to the regulation of MYB and WRKY transcription signals, as well as an increased supply of primary metabolic precursors from enhanced photosynthesis. A simplified schematic diagram of this interaction is shown in Fig. 10. The present results deepen our understanding of the molecular mechanisms of plant-microbe interactions. The proposed Ca^{2+}-kinase cascade transcription factor regulation model provides a clear research framework for further in-depth analysis of how microbial signals are perceived and converted into metabolic responses by plants. This study confirms the enormous potential of using specific endophytes, especially fungus F9, as microbial agents to simultaneously increase the yield and medicinal quality of *A. lancea* in a green and sustainable manner. This provides new technical ideas for the standardized cultivation and quality improvement of medicinal plants. This study still has certain limitations. The currently proposed regulatory models are mainly based on omics data and component association analysis, and their precise molecular details still need to be further validated through genetic and molecular biology experiments.

Author contributions

The authors confirm their contributions to the paper as follows: performed the experiments, processed and analyzed data, and composed the draft version of the manuscript: Guo X and Zhang C; investigation, conceptualization, supervision, project administration: Wang H, Kang C, and Guo L; funding acquisition: Guo L, Wang H, Kang C, Zhang Y, and Wang S. All authors provided assistance and valuable suggestions during the research execution, and on each version of the manuscript. All authors reviewed the results and approved the final version of the manuscript.

Data availability

The raw transcriptomic data have been uploaded to the National Genomics Data Center (https://ngdc.cncb.ac.cn/), with accession ID CRA029373. The other data generated or analyzed during this study are included in this published article and its supplementary information files. Further enquiries can be directed to the corresponding authors.

Conflict of interest

The authors declare that they have no conflict of interest.

References

1. Jiang L, Chen Y, Wang X, Guo W, Bi Y, et al. 2022. New insights explain that organic agriculture as sustainable agriculture enhances the sustainable development of medicinal plants. *Frontiers in Plant Science* 13:959810
2. He L, Zhang S, Yang C, Xu B, Su Z, et al. 2021. 生态扶贫视域下的中药材生态种植论析 [Ecological planting of Chinese medicinal materials from perspective of ecological poverty alleviation view]. *中国现代中药 [Modern Chinese Medicine]* 23:417−20 (in Chinese)

3. Wang Y, Zhang Y, Cong H, Li C, Wu J, et al. 2023. Cultivable endophyte resources in medicinal plants and effects on hosts. *Life* 13:1695

4. Lv J, Yang S, Zhou W, Liu Z, Tan J, et al. 2024. Microbial regulation of plant secondary metabolites: Impact, mechanisms and prospects. *Microbiology Research* 283:127688

5. Zhang WJ, Zhao ZY, Chang LK, Cao Y, Wang S, et al. 2021. Atractylodis Rhizoma: a review of its traditional uses, phytochemistry, pharmacology, toxicology and quality control. *Journal of Ethnopharmacology* 266:113415

6. Gu Y, Feng X, Xia B. 2007. Dynamic change of essential oil content and increment in different organs of *Atractylodes lancea*. *Journal of Plant Resources and Environment* 16:24−28, 42

7. Ouyang L. 2023. *Study on the grade standard of Atractylodis Rhizoma.* Thesis. Shanghai University of Traditional Chinese Medicine, China. pp. 15-24 doi: 10.27320/d.cnki.gszyu.2020.000736

8. Chen LJ, Wu XQ, Xu Y, Wang BL, Liu S, et al. 2021. Microbial diversity and community structure changes in the rhizosphere soils of *Atractylodes lancea* from different planting years. *Plant Signaling & Behavior* 16:1854507

9. Wu H, Lin W. 2020. 药用植物连作障碍研究评述和发展透视 [A commentary and development perspective on the consecutive monoculture problems of medicinal plants]. 中国生态农业学报 [*Chinese Journal of Eco-Agriculture*] 28:775−93

10. Wang H, Wang Y, Kang C, Wang S, Zhang Y, et al. 2022. Drought stress modifies the community structure of root-associated microbes that improve *Atractylodes lancea* growth and medicinal compound accumulation. *Frontiers in Plant Science* 13:1−19

11. Fang F, Dai C, Zhang B, Liang Q. 2009. 茅苍术悬浮细胞系建立及内生真菌诱导子对其挥发油积累的影响 [Establishment of suspension cell line of *At ractylodes lancea* and effect of endophytic fungal elicitors on its essential oil accumulation]. 中草药 [*Chinese Traditional and Herbal Drugs*] 40:452−55

12. Yang H. 2022. *Study on signal difference of endophytic bacteria promoting volatile oil accumulation in Atractylodes macrocephala and Atractylodes lancea.* Thesis. Nanjing Normal University, China. pp. 4−5 doi: 10.27245/d.cnki.gnjsu.2019.002423

13. Cao L, Chen F, Dai C. 2022. 茅苍术与内生菌互作信号对其活性成分的影响 [Change of *Atractylodes lancea* signaling during endogenous microbes colonization effects the genuine active compounds]. 农业环境科学学报 [*Journal of Agro-Environment Science*] 41:2831−39

14. Fang F, Dai C, Wang Y. 2009. 一氧化氮和过氧化氢在内生真菌小克银汉霉属 AL4 诱导子促进茅苍术细胞挥发油积累中的作用 [Role of nitric oxide and hydrogen peroxide in the essential oil increasing of suspension cells from *Atractylodes lancea* induced by endophytic fungal *Cunninghamella* sp. AL4 elicitor]. 生物工程学报 [*Chinese Journal of Biotechnology*] 25:1490−96

15. Wang XM, Yang B, Ren CG, Wang HW, Wang JY, et al. 2015. Involvement of abscisic acid and salicylic acid in signal cascade regulating bacterial endophyte-induced volatile oil biosynthesis in plantlets of *Atractylodes lancea*. *Plant Physiology* 153:30−42

16. Bai B, Liu W, Qiu X, Zhang J, Zhang J, et al. 2022. The root microbiome: Community assembly and its contributions to plant fitness. *Journal of Integrative Plant Biology* 64:230−43

17. Fan X, Ge AH, Qi S, Guan Y, Wang R, et al. 2025. Root exudates and microbial metabolites: signals and nutrients in plant-microbe interactions. *Science China Life Sciences* 68:2290−302

18. Srivastava AK, Singh RD, Pandey GK, Mukherjee PK, Foyer CH. 2025. Unravelling the molecular dialogue of beneficial microbe−plant interactions. *Plant Cell & Environment* 48:2534−48

19. Zeng Q, Hu HW, Ge AH, Xiong C, Zhai CC, et al. 2025. Plant−microbiome interactions and their impacts on plant adaptation to climate change. *Journal of Integrative Plant Biology* 67:826−44

20. Zhang C, Wang S, Sun J, Li X, Wang H, et al. 2024. Genome resequencing reveals the genetic basis of population evolution, local adaptation, and rewiring of the rhizome metabolome in *Atractylodes lancea*. *Horticulture Research* 11:uhae167

21. Love MI, Huber W, Anders S. 2014. Moderated estimation of fold change and dispersion for RNA-seq data with DESeq2. *Genome Biology* 15:550

22. Wu T, Hu E, Xu S, Chen M, Guo P, et al. 2021. clusterProfiler 4.0: a universal enrichment tool for interpreting omics data. *Innovation* 2:100141

23. Livak KJ, Schmittgen TD. 2001. Analysis of relative gene expression data using real-time quantitative PCR and the $2^{−\Delta\Delta CT}$ Method. *Methods* 25:402−8

24. Chen W, Gao Y, Xie W, Gong L, Lu K, et al. 2014. Genome-wide association analyses provide genetic and biochemical insights into natural variation in rice metabolism. *Nature Genetics* 46:714−21

25. Pang Z, Mao X, Zhou S, Yu S, Liu G, et al. 2023. Microbiota-mediated nitrogen fixation and microhabitat homeostasis in aerial root-mucilage. *Microbiome* 11:85

26. Thévenot EA, Roux A, Xu Y, Ezan E, Junot C. 2015. Analysis of the human adult urinary metabolome variations with age, body mass index, and gender by implementing a comprehensive workflow for univariate and OPLS statistical analyses. *Journal of Proteome Research* 14:3322−35

27. Jeon JE, Kim JG, Fischer CR, Mehta N, Dufour-Schroif C, et al. 2020. A pathogen-responsive gene cluster for highly modified fatty acids in tomato. *Cell* 180:176−187.e19

28. Li KP, Yuan M, Wu YL, Pineda M, Zhang CM, et al. 2022. A high-fat high-fructose diet dysregulates the homeostatic crosstalk between gut microbiome, metabolome, and immunity in an experimental model of obesity. *Molecular Nutrition & Food Research* 66:e2100950

29. Yuan J. 2019. *The mechanism of endophytic fungus Gilmaniella sp. AL12 promotion of plant growth and sesquiterpenoid accumulation in Atractylodes lancea.* Thesis. Nanjing Normal University, China. pp. 4-6 doi: 10.27245/d.cnki.gnjsu.2019.002436

30. Sun XL, Xu YF, Ma LY, Zhou H. 2010. 植株叶片的光合色素构成对遮阴的响应 [A review of acclimation of photosynthetic pigment composition in plant leaves to shade environment]. 植物生态学报 [*Chinese Journal of Plant Ecology*] 34:989−99

31. Pandey SS, Singh S, Pandey H, Srivastava M, Ray T, et al. 2018. Endophytes of *Withania somnifera* modulate in planta content and the site of withanolide biosynthesis. *Scientific Reports* 8:5450

32. Hou S, Thiergart T, Vannier N, Mesny F, Ziegler J, et al. 2021. A microbiota-root-shoot circuit favours *Arabidopsis* growth over defence under suboptimal light. *Nature Plants* 7:1078−92

33. Zhou J. 2016. *Mechanisms underlying Pseudomonas fluorescens efficiently increasing the sesquiterpenoid content and diversity in Atractylodes lancea.* Thesis. Nanjing Normal University, China. pp. 4−7

34. Xu S, Dong H, Zeng X, Zhao Z. 2019. 萜类植物源农药的筛选及活性研究进展 [Research progress in screening and bioactivity of terpenoid botanical pesticides]. 林产化学与工业 [*Chemistry and Industry of Forest Products*] 39:1−12

35. Ren CG, Dai CC. 2012. Jasmonic acid is involved in the signaling pathway for fungal endophyte-induced volatile oil accumulation of *Atractylodes lancea* plantlets. *BMC Plant Biology* 12:128

36. Ren CG, Dai CC. 2013. Nitric oxide and brassinosteroids mediated fungal endophyte-induced volatile oil production through protein phosphorylation pathways in *Atractylodes lancea* plantlets. *Journal of Integrative Plant Biology* 55:1136−46

37. Cui X, Zhao P, Liang W, Cheng Q, Mu B, et al. 2020. A rapeseed WRKY transcription factor phosphorylated by CPK modulates cell death and Leaf senescence by regulating the expression of ROS and SA-synthesis-related genes. *The Journal of Agricultural and Food Chemistry* 68:7348−59

38. Gao X, He P. 2013. Nuclear dynamics of *Arabidopsis* calcium-dependent protein kinases in effector-triggered immunity. *Plant Signaling & Behavior* 8:e23868

39. Wang D, Wei L, Liu T, Ma J, Huang K, et al. 2023. Suppression of ETI by PTI priming to balance plant growth and defense through an MPK3/MPK6-WRKYs-PP2Cs module. *Molecular Plant* 16:903−18

40. Hao X, Wang S, Fu Y, Liu Y, Shen H, et al. 2024. The WRKY46-MYC2 module plays a critical role in E-2-hexenal-induced anti-herbivore responses by promoting flavonoid accumulation. *Plant Communications* 5:100734

41. Kazan K, Manners JM. 2013. MYC2: the master in action. *Molecular Plant* 6:686−703

42. Zheng H, Fu X, Shao J, Tang Y, Yu M, et al. 2023. Transcriptional regulatory network of high-value active ingredients in medicinal plants. *Trends in Plant Science* 28:429−46

43. Wang L, Chen M, Lam PY, Dini-Andreote F, Dai L, et al. 2022. Multi-faceted roles of flavonoids mediating plant-microbe interactions. *Microbiome* 10:233

44. Hartwig UA, Joseph CM, Phillips DA. 1991. Flavonoids released naturally from alfalfa seeds enhance growth rate of *Rhizobium meliloti*. *Plant Physiology* 95:797−803

45. Zhang J, Subramanian S, Stacey G, Yu O. 2009. Flavones and flavonols play distinct critical roles during nodulation of *Medicago truncatula* by *Sinorhizobium meliloti*. *Plant Journal* 57:171−83

46. Begum N, Wang L, Ahmad H, Akhtar K, Roy R, et al. 2022. Co-inoculation of arbuscular mycorrhizal fungi and the plant growth-promoting rhizobacteria improve growth and photosynthesis in tobacco under drought stress by up-regulating antioxidant and mineral nutrition metabolism. *Microbial Ecology* 83:971−88

47. Okutani F, Hamamoto S, Aoki Y, Nakayasu M, Nihei N, et al. 2020. Rhizosphere modelling reveals spatiotemporal distribution of daidzein shaping soybean rhizosphere bacterial community. *Plant Cell & Environment* 43:1036−46

48. Schütz V, Frindte K, Cui J, Zhang P, Hacquard S, et al. 2021. Differential impact of plant secondary metabolites on the soil microbiota. *Frontiers in Microbiology* 12:666010

49. Yu P, He X, Baer M, Beirinckx S, Tian T, et al. 2021. Plant flavones enrich rhizosphere *Oxalobacteraceae* to improve maize performance under nitrogen deprivation. *Nature Plants* 7:481−99

50. Wang M, Qiu X, Pan X, Li C. 2021. Transcriptional factor-mediated regulation of active component biosynthesis in medicinal plants. *Current Pharmaceutical Biotechnology* 22:848−66